

Two new species of *Calonectria* (Hypocreales, Nectriaceae) causing *Eucalyptus* leaf blight in Brazil

Enrique I. Sanchez-Gonzalez¹, Thaissa de Paula Farias Soares²,
Talyta Galafassi Zarpelon², Edival Angelo Valverde Zauza²,
Reginaldo Gonçalves Mafia², Maria Alves Ferreira¹

¹ Universidade Federal de Lavras, Departamento de Fitopatologia, Lavras, MG, 37200-900, Brasil ² Suzano Papel e Celulose S. A. Centro de Tecnologia, Aracruz, ES, 29197-900, Brasil

Corresponding author: Maria Alves Ferreira (mariaferreira@ufla.br)

Academic editor: Nalin Wijayawardene | Received 5 April 2022 | Accepted 29 June 2022 | Published 29 July 2022

Citation: Sanchez-Gonzalez EI, Farias Soares TdP, Galafassi Zarpelon T, Valverde Zauza EA, Gonçalves Mafia R, Alves Ferreira M (2022) Two new species of *Calonectria* (Hypocreales, Nectriaceae) causing *Eucalyptus* leaf blight in Brazil. MycoKeys 91: 169–197. <https://doi.org/10.3897/mycokeys.91.84896>

Abstract

In recent decades, commercial *Eucalyptus* plantations have expanded toward the warm and humid regions of northern and northeastern Brazil, where *Calonectria* leaf blight (CLB) has become the primary fungal leaf disease of this crop. CLB can be caused by different *Calonectria* species, and previous studies have indicated that *Calonectria* might have high species diversity in Brazil. During a disease survey conducted in three commercial plantations of *Eucalyptus* in northeastern Brazil, diseased leaves from *Eucalyptus* trees with typical symptoms of CLB were collected, and *Calonectria* fungi were isolated. Based on phylogenetic analyses of six gene regions (*act*, *cmdA*, *bis3*, *rpb2*, *tef1*, and *tub2*) and morphological characteristics, two new species of *Calonectria* were identified. Five isolates were named as *C. paragominensis* sp. nov. and four were named as *C. imperata* sp. nov. The pathogenicity to *Eucalyptus* of both species was confirmed by fulfilling the Koch's postulates.

Keywords

Cylindrocladium, GCPSR, phylogenetic network analysis, phylogeny

Introduction

Calonectria species are widely distributed around the world and cause diseases in more than 335 plant species, distributed among nearly 100 plant families, including forestry, agricultural and horticultural crops (Crous 2002; Lombard et al. 2010c; Vitale et al. 2013; Lombard et al. 2016; Li et al. 2021). Most reports of *Calonectria* from Brazil are focused on forestry crops, such as *Acacia*, *Eucalyptus*, and *Pinus* trees (Alfenas et al. 2015), and mainly evaluate the epidemiology and disease control of *Calonectria*-associated diseases such as *Calonectria* leaf blight (CLB), damping-off, cutting rot and root rot in commercial plantations and nurseries of *Eucalyptus* (Soares et al. 2018).

Currently, 130 *Calonectria* species have been identified based on DNA phylogenetic analyses and morphological comparisons (Crous et al. 2018, 2019, 2021a, 2021b; Wang et al. 2019; Liu et al. 2020; Mohali and Stewart 2021; Pham et al. 2022). These species are accommodated in eleven species complexes, which are divided into two main phylogenetic groups based on their morphological features: the Prolate Group (*C. brasicaceae*, *C. candelabrum*, *C. colhounii*, *C. cylindrospora*, *C. gracilipes*, *C. mexicana*, *C. pteridis*, *C. reteaudii* and *C. spathiphylli* species complexes), and the Sphaero-Naviculate Group (*C. kyotensis* and *C. naviculata* species complexes) (Lombard et al. 2016; Liu et al. 2020).

In Brazil, a total of 35 species have been described: eleven species isolated from diseased tissues of *Eucalyptus*, ten species isolated from soil samples of *Eucalyptus* plantations, seven species isolated from different plant species, six species isolated from soil samples of tropical rainforests, and one mycoparasite species (Crous et al. 2018, 2019; Liu et al. 2020); they belong in the species complexes of *C. candelabrum*, *C. brassicaceae*, *C. cylindrospora*, *C. pteridis*, *C. gracilipes*, and *C. naviculata* (Crous et al. 2018, 2019; Liu et al. 2020). The results from a previous study indicated high species diversity of *Calonectria* in Brazil (Alfenas et al. 2015).

Brazil is one of the main producers of pulp, paper, and wood panels in the world, mainly due to the genus *Eucalyptus*; its hybrids are the most grown trees in the country for these purposes (IBÁ, 2021). In 2020, the total area of *Eucalyptus* plantations was 7.47 million hectares, with an average productivity of 36.8 m³/ha per year (IBÁ, 2021). However, in recent decades, commercial *Eucalyptus* plantations have expanded toward the warm and humid regions of northern and northeastern Brazil, where CLB has become the primary fungal leaf disease of this crop (Alfenas et al. 2015). CLB can be caused by different *Calonectria* species, is widely distributed throughout the country, and affects *Eucalyptus* plants most severely from six months to 2–3 years after planting (Graça et al. 2009). This disease starts from spores or microsclerotia present in soil or diseased plant debris on the ground and disseminates to lower branches of the tree canopy; lesions start at the base, apex or margins of leaves and can reach a large area of the leaf blade, resulting in leaf drop and, in some cases, severe defoliation in the basal, middle, and apical thirds of the canopy (Alfenas et al. 2009). The defoliation may decrease timber volume as a result of the reduced photosynthetic area and facilitates weed growth due to the increased entrance of light through the subcanopy, leading to competition for nutrients between *Eucalyptus* and understory plants (Graça et al. 2009; Alfenas et al. 2015).

CLB can be controlled by integrated cultivation and chemical methods as well as by the selection and cultivation of resistant genotypes, which is a much more effective approach (Soares et al. 2018). The demand for new strategies to control this disease requires proper identification of the pathogen species. Additionally, this information may be useful for breeding programs, leading to the development of *Eucalyptus* genotypes resistant to CLB. Recently, during a disease survey conducted in three commercial plantations of *Eucalyptus* in northeastern Brazil, diseased leaves from *Eucalyptus* trees with typical symptoms of CLB were collected, and *Calonectria* fungi were isolated. Thus, the aims of this study were to identify these isolates based on phylogenetic analyses and morphological characteristics and to confirm their pathogenicity to *Eucalyptus*.

Materials and methods

Sample collection and fungal isolation

In February 2020, during a disease survey conducted in three commercial plantations of *Eucalyptus* on six-month-old to one-year-old trees, diseased leaves with typical symptoms of CLB (small, circular or elongated pale grey to pale brown to dark brown spots, that extend throughout the leaf blade), were observed and collected for fungal isolation and species characterization. On average, 50 diseased leaves were sampled from each *Eucalyptus* genotype, one leaf per tree, depending on the planted areas. The sampled *Eucalyptus* genotypes corresponded to *E. urophylla*, localized in the municipalities of Cidelândia ($5^{\circ}09'24"S$, $47^{\circ}46'26"W$) and Itinga do Maranhão ($4^{\circ}34'43"S$, $47^{\circ}29'48"W$), in the state of Maranhão, and to the *E. grandis* × *E. brassiana* hybrid genotype, in the microregion of Paragominas ($3^{\circ}10'51"S$, $47^{\circ}18'49"W$), in the state of Pará, Brazil.

Samples were stored in paper bags and transported to the Laboratory of Forest Pathology at the Universidade Federal de Lavras. From each leaf, small segments of 1 cm² from the transition section between healthy and diseased tissue were cut and the surface was disinfected by washing with 1% sodium hypochlorite for 1 min, with 70% ethanol for 30 s and with sterilized water three times before culture on 2% malt extract agar (MEA; malt extract 20 g·L⁻¹, agar 20 g·L⁻¹, yeast extract 2 g·L⁻¹, sucrose 5 g·L⁻¹) plates at 25 °C. After 48 h of incubation, *Calonectria*-like mycelial plugs, 5 mm in diameter, were transferred to a fresh MEA plate and incubated at 25 °C until the fungus covered the plate completely. Induction of sporulation on MEA plates and single spore cultures was obtained following the procedures described by Alfenas et al. (2013). Each single spore culture was stored and maintained in a metabolically inactive state in dry culture and sterile water following Castellani's method (Castellani 1939). Holotypes were deposited as herbaria in the Coleção Micológica do Herbário da Universidade de Brasília (UB). Ex-types were deposited as pure cultures in the Coleção de Culturas de Microrganismos do Departamento de Ciência dos Alimentos/UFLA (CCDCA) at Universidade Federal de Lavras (UFLA), Minas Gerais, Brazil. Ex-paratypes were deposited as pure cultures in the Laboratory of Forest Pathology (PFC) at UFLA.

DNA extraction, PCR amplification, and sequencing

Total genomic DNA was extracted from fresh mycelia of single spore cultures grown on malt extract broth (MEB; malt extract 20 g·L⁻¹, yeast extract 2 g·L⁻¹, sucrose 5 g·L⁻¹) for ten days at 25 °C in the dark. The protocol described by Lee and Taylor (1990) was followed with slight modifications; by adding 1.5 M NaCl and 2% polyvinylpyrrolidone (MW: 40000) to the lysis buffer; the DNA was precipitated directly with isopropanol without the use of 3 M NaOAc, and the DNA pellet was dried at room temperature overnight. A NanoDrop 1,000 spectrometer (Thermo Fisher Scientific, Waltham, MA, USA) was used to quantify its concentration.

Based on a previous study (Liu et al. 2020), actine (*act*), calmodulin (*cmdA*), histone H3 (*his3*), RNA polymerase II (*rpb2*), translation elongation factor 1-alpha (*tef1*), and β-tubulin (*tub2*) genes were used as DNA barcodes due to provide a stable and reliable resolution to distinguish all *Calonectria* species. The primers ACT-512F and ACT-783R (Carbone and Kohn 1999) were used to amplify the *act* gene region; CAL-228F and CAL-2Rd (Carbone and Kohn 1999; Quaedvlieg et al. 2011) for the *cmdA* gene region; CYLH3F and CYLH3R (Crous et al. 2004) for the *his3* gene region; fRpb2-5F and fRpb2-7cR (Liu et al. 1999; Reeb et al. 2004) for the *rpb2* gene region; EF1-728F (Carbone and Kohn 1999) and EF2 (O'Donnell et al. 1998) for the *tef1* gene region and the primer pairs T1 (O'Donnell and Cigelnik 1997) and CYLTUB1R (Crous et al. 2004) for the *tub2* gene region.

The PCRs were carried out in a 25 µL final volume containing molecular biology-grade water (Sigma–Aldrich, St. Louis, MO, USA) 1X PCR buffer (Promega, Madison, WI, USA), 2.5 mM MgCl₂, 0.2 mM deoxyribonucleotide triphosphate (dNTP) mix (Promega, Madison, WI, USA), 1 U GoTaq Flexi DNA Polymerase (Promega, Madison, WI, USA), 0.2 mM each primer, and 30 ng DNA template. DNA amplifications were conducted in a thermal cycler (5 PRIME G gradient Thermal Cycler, Techne, Staffordshire, UK). The PCR conditions for the *act*, *cmdA*, *his3*, *tef1*, and *tub2* gene regions were as follows: an initial denaturation step at 95 °C for 5 min; then 35 amplification cycles at [94 °C for 30 s; 52 °C for 1 min; 72 °C for 2 min], and a final extension step at 72 °C for 5 min. For the *rpb2* gene region, a touchdown PCR protocol was used: an initial denaturation step at 95 °C for 5 min, then (95 °C for 30 s, 57 °C for 30 s, 72 °C for 90 s) × 10 cycles, (95 °C for 30 s, 57 °C for 45 s, 72 °C for 90 s + 5 s/cycle increase) × 30 cycles, and a final extension step at 72 °C for 10 min.

PCR products were separated by electrophoresis at 120 V for 1 h in a 1.2% agarose gel, stained with Diamond Nucleic Acid Dye (Promega, Madison, WI, USA), and visualized using an ultraviolet light transilluminator. Successful PCR products were purified and sequenced in both directions using the same primer pairs used for amplification by Macrogen Inc. (Macrogen, Seoul, Korea). Raw sequences from each gene region were edited, consensus sequences were generated using SeqAssem software ver. 07/2008 (Hepperle 2004), and the sequences generated in this study were deposited in the NCBI/GenBank database (<http://www.ncbi.nlm.nih.gov>).

Phylogenetic analyses

The generated sequences were aligned with other sequences of closely related *Calonectria* spp. obtained from GenBank (Table 1), using the online interface of MAFFT v. 7.0 (Katoh et al. 2019, <http://mafft.cbrc.jp/alignment/server>) with the alignment strategy FFT-NS-i (Slow; interactive refinement method). Alignments were manually corrected using MEGA7 (Kumar et al. 2016).

The partition homogeneity test (PHT) described by Farris et al. (1995) was conducted to determine if data for six genes could be combined using PAUP 4.0b10 (Swofford 2003). To determine the phylogenetic relationships among species, phylogenetic analyses based on maximum parsimony (MP), maximum likelihood (ML), and bayesian inference (BI) were conducted on the individual gene regions and their concatenated dataset, depending on the sequence availability.

Maximum parsimony analysis was performed using PAUP 4.0b10 (Swofford 2003), with phylogenetic relationships estimated by heuristic searches, random step-wise addition sequences, and tree bisection and reconnection (TBR) branch swapping. Gaps were treated as missing data, and all characters were unordered and weighted equally. The measures calculated for parsimony included the tree length (TL), consistency index (CI), homoplasy index (HI), retention index (RI), and rescaled consistency index (RC). Statistical support for branch nodes was assessed with 1,000 bootstrap replicates.

The best evolutionary model of nucleotide substitution for each gene region was selected according to the Akaike Information Criterion (AIC) using MODELTEST v. 3.4 (Posada and Crandall 1998) for ML analyses and MRMODELTEST v. 2 (Nylander 2004) for BI analyses.

ML analyses for individual gene regions were performed using PAUP 4.0b10 (Swofford 2003). The ML models used were K80 + G (*act*), TVM + G (*cmdA*), TrN + G (*his3*), SYM + G (*rpb2*), TVM + I + G (*tef1*) and HKY + I (*tub2*). Statistical support for branch nodes was assessed with 1,000 bootstrap replicates. A partitioned ML analysis was performed using IQ-TREE (Nguyen et al. 2015) as implemented in the IQ-TREE web server (<http://iqtree.cibiv.univie.ac.at>, Trifinopoulos et al. 2016) by using partition models (Chernomor et al. 2016). Branch support values were evaluated based on 10,000 replicates for ultrafast bootstrapping (UFBoot2) (Hoang et al. 2018).

Individual and partitioned BI analyses were performed using MRBAYES v.3.2.7a (Ronquist et al. 2012) on XSEDE at the CIPRES Science Gateway v.3.3 (<http://www.phylo.org/>). The BI models used were K80 + G (*act*), GTR + G (*cmdA* and *his3*), SYM + G (*rpb2*), GTR + I + G (*tef1*) and HKY + I (*tub2*). A Markov Chain Monte Carlo (MCMC) algorithm was employed, and two independent runs of four MCMC chains (three hot and one cold) were run in parallel simultaneously starting from random trees for 10^7 generations (individual gene regions) and 30^7 generations (concatenated dataset), sampling trees every 1,000 generations. The distribution of log-likelihood scores was examined with TRACER v.1.5 (Rambaut and Drummond 2007) to determine the whether the stationary phase of each search was reached and whether chains

Table 1. *Calonectria* species and GenBank accession numbers of DNA sequences used in this study.

Species complex	Species	Isolate representing the species [§]	Other isolate numbers	Host/ Substrate	Country	Genbank accession numbers					
						<i>act</i> [†]	<i>cndA</i>	<i>bis3</i>	<i>rpb2</i>	<i>tfl1</i>	<i>tb2</i>
<i>Calonectria</i> <i>spathiphylli</i> species complex	<i>C. densa</i>	CMW 311182		Soil	Ecuador	GQ280525	GQ267444	GQ267281	N/A	GQ267352	GQ267232
		CMW 311184		Soil	Ecuador	GQ280523	GQ267442	GQ267279	N/A	GQ267350	GQ267230
		CMW 311185		Soil	Ecuador	GQ280524	GQ267443	GQ267280	N/A	GQ267351	GQ267231
CMW 311183				Soil	Ecuador	GQ280526	GQ267445	GQ267282	N/A	GQ267353	GQ267233
CMW 311186				Soil	Ecuador	GQ280527	GQ267446	GQ267283	N/A	GQ267354	GQ267234
CMW 311187				Soil	Ecuador	GQ280528	GQ267447	GQ267284	N/A	GQ267355	GQ267235
<i>C. paragominensis</i> sp. nov. [†]		<i>E. brasiliensis</i>		Brazil	ON009346	OM974325	OM974334	OM974343	OM974352	OM974361	
		<i>E. granadis</i> × <i>E. brasiliensis</i>		Brazil	ON009347	OM974326	OM974335	OM974344	OM974353	OM974362	
		<i>E. granadis</i> × <i>E. brasiliensis</i>		Brazil	ON009348	OM974327	OM974336	OM974345	OM974354	OM974363	
		<i>E. granadis</i> × <i>E. brasiliensis</i>		Brazil	ON009349	OM974328	OM974337	OM974346	OM974355	OM974364	
		<i>E. granadis</i> × <i>E. brasiliensis</i>		Brazil	ON009350	OM974329	OM974338	OM974347	OM974356	OM974365	
<i>C. pseudospathiphylli</i>	CBS 109165	CPC 1623		Soil	Ecuador	GQ280493	GQ267412	AF348241	KY653435	FJ918562	AF348225
		CPC 1641		Soil	Ecuador	N/A	N/A	AF348233	N/A	N/A	AF348217
<i>C. spathiphylli</i>	CBS 114540	ATCC4730, CSF11330	<i>Spathiphyllum</i> sp.	USA	GQ280505	GQ267424	AF348230	MT412666	GQ267330	AF348214	
		CSF 11401	<i>Spathiphyllum</i> sp.	Switzerland	GQ280506	GQ267425	FJ918530	MT412667	FJ918561	FJ918512	
<i>Calonectria</i> <i>candelabrum</i> species complex	<i>C. brasiliensis</i>	CBS 1111484	CSF 11249	Soil	Brazil	MT334968	MT335198	MT335438	MT412502	MT412729	MT412951
		CBS 1111485	CSF 11250	Soil	Brazil	MT334969	MT335199	MT335439	MT412503	MT412730	MT412952
		CBS 134855		Soil	Brazil	N/A	KM396056	KM396139	N/A	KM395882	KM395969
		CBS 134856		Soil	Brazil	N/A	KM396057	KM396140	N/A	KM395883	KM395970
		CBS 115671	CSC 11288	Soil	Mexico	MT334973	MT335203	MT335443	MT412507	MT412734	MT412956
		CBS 110928	CSF 11235	Soil	Mexico	MT334974	MT335204	MT335444	MT412508	MT412735	MT412957
<i>C. candelabrum</i>	CMW 31000	CSF 11404	<i>Eucalyptus</i> sp.	Brazil	MT334977	MT335207	MT335447	MT412511	MT412738	MT412959	
		CMW 31001	<i>Eucalyptus</i> sp.	Brazil	MT334978	MT335208	MT335448	MT412512	MT412739	MT412960	
		CSF 11405		Soil	Colombia	GQ280538	GQ267455	FJ972442	N/A	FJ972492	FJ972423
		CBS 115127		Soil	Colombia	GQ280539	GQ267456	FJ972441	N/A	FJ972491	FJ972422
		<i>C. brevistipitata</i>		<i>Eucalyptus</i> sp.	Brazil	N/A	KM396051	KM396134	N/A	KM395877	KM395964
		<i>C. candelabrum</i>		<i>Eucalyptus</i> sp.	Brazil	N/A	KM396050	KM396133	N/A	KM395876	KM395963
		<i>C. colombiana</i>		<i>Fragaria × ananassa</i>	Brazil	N/A	KM998966	KM998964	N/A	KM998963	KM998965
		<i>C. eucalyptola</i>		<i>Fragaria × ananassa</i>	Brazil	N/A	KX500191	KX500194	N/A	KX500197	KX500195
		<i>C. fragariae</i>		<i>Eucalyptus</i> sp.	Brazil	N/A	KM396053	KM396136	N/A	KM395879	KM395966
		<i>C. glacicola</i>		<i>Eucalyptus</i> sp.	Brazil	N/A	KM396054	KM396137	N/A	KM395880	KM395967
		<i>C. hemileiae</i>		<i>Hemileia vastatrix</i>	Brazil	N/A	MK037392	MK006026	N/A	MK006027	MK037391

Species complex	Species	Isolate representing the species [§]	Other isolate numbers	Host/ Substrate	Country	Genbank accession numbers				
						<i>act</i> [†]	<i>cndA</i>	<i>his3</i>	<i>rpb2</i>	<i>tef1</i>
<i>Calonectria candelabrum</i> species complex	<i>C. imperata</i> sp. nov. [‡]	CCDCA 11649		<i>E. urophylla</i>	Brazil	ON009351	OM974330	OM974339	OM974348	OM974357
		PFC7		<i>E. urophylla</i>	Brazil	ON009352	OM974331	OM974340	OM974349	OM974358
		PFC8		<i>E. urophylla</i>	Brazil	ON009353	OM974332	OM974341	OM974350	OM974359
		PFC9		<i>E. urophylla</i>	Brazil	ON009354	OM974333	OM974342	OM974351	OM974360
	<i>C. matogrossensis</i>	GFP 006		<i>E. urophylla</i>	Brazil	N/A	MH1837653	MH1837648	N/A	MH1837659
		GFP 018		<i>E. urophylla</i>	Brazil	N/A	MH1837657	MH1837652	N/A	MH1837663
<i>C. metroisideri</i>	CBS 133603	CSF 11309	<i>Metridiosporomycophora</i>	Brazil	N/A	KC294307	KC294304	N/A	KC294310	KC294313
		CBS 133604	<i>Metridiosporomycophora</i>	Brazil	MT335056	MT335288	MT335288	MT412810	MT413033	
<i>C. nemoricola</i>	CBS 134837		Soil	Brazil	N/A	KM396066	KM396149	N/A	KM395892	KM395979
		CBS 134838	Soil	Brazil	N/A	KM396067	KM396150	N/A	KM395893	KM395980
<i>C. pauciramosa</i>	CBS 138324	CSF 16461	Soil	South Africa	MT335093	MT335325	MT335365	MT412618	MT413068	
		CMW 3147/4	<i>E. urophylla</i> × <i>E. grandis</i>	China	MT335104	MT335336	MT335576	MT412629	MT413079	
<i>C. piauiensis</i>	CBS 134850	CSF 11422		Soil	Brazil	N/A	KM396060	KM396143	N/A	KM395886
		CBS 134851		Soil	Brazil	N/A	KM396061	KM396144	N/A	KM395887
<i>C. pseudometroisideri</i>	CBS 134845		Soil	Brazil	N/A	KM395995	KM396083	N/A	KM395821	KM395909
		CBS 134843	<i>Metridiosporomycophora</i>	Brazil	N/A	KM395993	KM396081	N/A	KM395819	KM395907
<i>C. pseudospathulata</i>	CBS 134841		Soil	Brazil	N/A	KM396070	KM396153	N/A	KM395896	KM395973
		CBS 134840		Soil	Brazil	N/A	KM396069	KM396152	N/A	KM395895
<i>C. putramosa</i>	CBS 111449	CSF 11246	<i>Eucalyptus</i> cutting	Brazil	MT335129	MT335364	MT335604	MT412657	MT413105	
		CBS 111470	Soil	Brazil	MT335130	MT335365	MT335605	MT412658	MT413106	
<i>C. siticola</i>	CBS 135237	LPF081	Soil	Brazil	N/A	KM396065	KM396148	N/A	KM395891	KM395978
		CBS 134836	Soil	Brazil	N/A	KM396062	KM396145	N/A	KM395888	KM395975
<i>C. spathulata</i>	CMW 16744	CSF 11331	<i>E. viminalis</i>	Brazil	MT335139	MT335376	MT335616	MT412668	MT412907	MT413117
		CBS 112513	<i>Eucalyptus</i> sp.	Colombia	MT335140	MT335377	MT335617	MT412669	MT412908	MT413118
<i>C. venezuelana</i>	CBS 111052	CSF 11238	Soil	Venezuela	MT335155	MT335394	MT335634	MT412685	MT412925	MT413132
		CSF 11289	Soil	Colombia	MT335022	MT335252	MT335492	MT412554	MT412783	MT413001
<i>Calonectria gracilipes</i> species complex	CBS 115674	CSF11239	Soil	Colombia	MT335023	MT335253	MT335493	MT412555	MT412784	MT413002

[†] New *Calonectria* species reported in the present study.

[‡] Ex-type isolates of the *Calonectria* species are marked in bold.

§ ATCC: American Type Culture Collection, Virginia, USA; CBS: Westerdijk Fungal Biodiversity Institute, Utrecht, The Netherlands; CCDCA: Coleção de Culturas de Microrganismos do Departamento de Ciências dos Alimentos/UFLA, Lavras, Brazil; CMW: Culture collection of the Forestry and Agricultural Biotechnology Institute (FABI), University of Pretoria, Pretoria, South Africa; COAD: Coleção Octávio de Almeida Drumond, Universidade Federal de Viçosa, Viçosa, Brazil; CPC: Pedro Crous working collection housed at Westerdijk Fungal Biodiversity Institute; CSF: Culture Collection located at China Eucalypt Research Centre (CERC), Chinese Academy of Forestry, Zhanjiang, GuangDong Province, China; GPF: Universidade Federal de Brasília, Brasília, Brazil; LPF: Laboratório de Patologia Florestal, Universidade Federal de Viçosa, Viçosa, Brazil; PFC: Laboratório de Patologia Florestal, Universidade Federal de Lavras, Lavras, Brazil.

| act: actin; cndA: calmodulin; his3: histone H3; rpb2: the second largest subunit of RNA polymerase; tef1: translation elongation factor 1-alpha; tub2: β-tubulin. GenBank accession number obtained in this study are marked in bold.

had achieved convergence. The convergence of the chains was also assessed by the convergent diagnostics of the effective sampling site (ESS), the potential scale reduction factor (PSRF), and the average standard deviation of split frequencies (ASDSF) (Ronquist et al. 2019). The first 25% of saved trees were discarded as the “burn-in” phase, and posterior probabilities (PP) were computed using the remaining trees. Trees were visualized in FIGTREE v. 1.4.4 (Rambaut 2009) and edited in INKSCAPE v. 1.0 (<https://inkscape.org>).

Pairwise homoplasy index (PHI) test and phylogenetic network analysis

Phylogenetically closely related species were analyzed using the Genealogical Concordance Phylogenetic Species Recognition (GCPSR) model (as described by Taylor et al. 2000) by performing a pairwise homoplasy index (Φ_w) test (PHI) (Bruen et al. 2006). The PHI test was performed in SPLIT TREE4 v.4.16.1. (<https://uni-tuebingen.de>) (Huson and Bryant 2006) to determine the recombination level within phylogenetically closely related species. Only the gene regions that were available for all compared individuals were used. Gaps’ sites were excluded. Significant recombination was considered at a PHI index below 0.05 ($\Phi_w < 0.05$). The relationships between closely related taxa were visualized by constructing a phylogenetic network from the concatenated datasets using the LogDet transformation and the NeighborNet method; the resultant networks were displayed with the EqualAngle algorithm (Dress and Huson 2004). Bootstrap analysis was then conducted with 1,000 replicates.

Mating type and sexual compatibility test

The mating-type idiomorph of each *Calonectria* species isolate was determined through PCR by using the primer pairs Cal_MAT111_F/Cal_MAT111_R and Cal_MAT121_F/Cal_MAT121_R, which amplify the MAT1-1-1 and MAT1-2-1 genes using the protocol described by Li et al. (2020). Additionally, sexual compatibility tests were performed for all the single-spore isolates of both species on minimal salt agar (MSA; Guerber and Correll 2001) by crossing them in all possible combinations, following the procedure described by Lombard et al. (2010a). The plates were stacked in plastic bags and incubated at 25 °C for 12 weeks.

Morphology

Morphological characterization of representative isolates of each *Calonectria* species identified by phylogenetic analyses was performed as described by Liu and Chen (2017). Optimal growth temperatures were determined by incubating the representative isolate at temperatures ranging from 5 °C to 30 °C at 5 °C intervals in the dark on MEA plates (three replicates per isolate were used). Colonial characteristics (diameter, color, and texture of colonies) were determined by inoculating the isolates on MEA plates at 25 °C in the dark after seven days of incubation.

Pathogenicity tests

One representative isolate of each *Calonectria* species was selected for inoculation. Healthy leaves of three short cut branches from an approximately eleven-month-old *Eucalyptus* plants were inoculated with suspensions of 1×10^4 conidia·mL⁻¹ obtained from single spore cultures. The conidia suspensions for each isolate were prepared using the method described by Graça et al. (2009). *Calonectria paragominensis* was inoculated on *E. grandis* × *E. brassiana* hybrid genotype and *C. imperata* on *E. urophylla* genotype. The inoculation consisted of spraying the conidia suspension until the suspension run off the leaves. Sterile water was sprayed onto healthy leaves as the negative control. The branches with inoculated leaves were covered with plastic bags to maintain high humidity and kept at 25 °C under a photoperiod of 12 h for 72 h. After that time, the plastic bags were removed, and necrotic symptoms were observed.

Results

Fungal isolates

A total of 34 isolates with the typical morphology of *Calonectria* species were obtained from infected leaves of the *Eucalyptus* genotypes sampled. Based on preliminary phylogenetic analyses of the *tef1* and *tub2* gene regions (data not shown), nine isolates were selected for further studies (Table 1).

Phylogenetic analyses

Sequences from 50 isolates corresponding to 25 *Calonectria* species closely related to the isolates obtained in this study were downloaded from GenBank (Table 1). For the nine isolates selected in this study, five resided in the *Calonectria spathiphylli* species complex (CSSC), and four resided in the *Calonectria candelabrum* species complex (CCSC). Both *Calonectria* complexes belong to the Prolate Group, whose species are characterized by their clavate to pyriform to ellipsoidal vesicles (Liu et al. 2020). Therefore, both complexes were combined into a single sequence dataset for phylogenetic analyses, including two strains of *Calonectria gracilipes* as the outgroup taxa.

Alignments for each gene region and the concatenated dataset were as follows: *act* (36 isolates, 267 characters), *cmdA* (58 isolates, 485 characters), *his3* (59 isolates, 439 characters), *rpb2* (28 isolates, 863 characters), *tef1* (58 isolates, 496 characters), *tub2* (59 isolates, 511 characters) and concatenated (59 isolates, 3061 characters). The PHT generated a *p* value of 0.01 for the concatenated dataset, suggesting some incongruence in the datasets for the six regions and the accuracy of the combined data could have suffered relative to the individual partitions (Cunningham 1997). Although the *p* value was low, the different gene regions were combined because the significance threshold

of 0.05 may be too conservative and it has been shown that combining incongruent datasets improves phylogenetic accuracy (Sullivan 1996; Cunningham 1997); moreover, this approach was followed by several previous studies (Lombard et al. 2016; Pham et al. 2019; Liu et al. 2020, 2021).

Tree topologies derived from the MP, ML, and BI analyses of the individual gene regions were similar overall, but the relative positions of some *Calonectria* species slightly differed. Moreover, the concatenated dataset formed well-supported lineages in the MP, ML, and BI analyses. Only the ML trees are presented in this study (Fig. 1, Suppl. material 1: Figs S1–S6). The concatenated dataset had 466 parsimony-informative characters, 67 parsimony-uninformative characters, and 2,528 constant characters. Analysis of the 466 parsimony-informative characters yielded 2 equally parsimonious trees, with TL = 862, CI = 0.7042, HI = 0.2958, RI = 0.9192, RC = 0.6472. For the partitioned BI analysis, the convergence of the chains was confirmed by an ESS > 200, a PSRF approaching 1, and an ASDSF equal to 0.000793. The aligned sequences were deposited in TreeBASE (<http://treebase.org>; No. 29573).

Phylogenetic analyses of the six individual gene regions showed that the five isolates from the CSSC were clustered in an independent clade (Suppl. material 1: Figs S1–S6). Based on the concatenated dataset of the six genes, the five isolates formed a new, strongly defined phylogenetic clade that was distinct from the other *Calonectria* species of the CSSC and was supported by high bootstrap values (MP = 100%, ML = 100%) and high values of posterior probability (1.0) (Fig. 1). A total of 41 fixed unique single nucleotide polymorphisms (SNPs) were identified in the new phylogenetic clade of the five isolates in comparison with their phylogenetically closely related *Calonectria* species in the six-gene concatenated dataset (Table 2). The results of these phylogenetic and SNP analyses indicate that the five isolates in the CSSC represent a distinct, undescribed species, which we named *C. paragominensis*.

Table 2. Single nucleotide polymorphisms unique to *C. paragominensis* in comparison with their phylogenetically closely related species in the six gene regions.

Species	<i>act</i> [†]												<i>cmd4</i>								
	188 [‡]	189	190	191	192	193	194	195	196	197	142	144	170	185	217	270	437	444	455	483	
<i>C. paragominensis</i> CCDCA 11648	a	g	a	a	a	a	a	g	a	a	t	a	c	c	t	c	a	a	g	a	
<i>C. densa</i> CMW 31182	t	-	-	-	-	-	-	-	-	-	a	c	t	t	c	t	g	g	a	c	
<i>C. humicola</i> CMW 31183	t	-	-	-	-	-	-	-	-	-	a	c	t	t	c	t	g	g	a	c	
<i>C. pseudospathiphylli</i> CBS 109165	t	-	-	-	-	-	-	-	-	-	a	c	t	t	c	t	g	g	a	c	
<i>C. spathiphylli</i> CBS 114540	t	-	-	-	-	-	-	-	-	-	a	c	t	t	c	t	g	g	a	c	
Species	<i>bis3</i>												<i>rpb2</i>								
	6	43	47	52	53	54	247	259	274	81	141	315	474	650	735	32	123	208	434	459	15
<i>C. paragominensis</i> CCDCA 11648	c	t	t	-	-	-	a	g	a	t	c	t	t	a	g	c	t	g	g	c	a
<i>C. densa</i> CMW 31182	t	a	c	c	t	c	t	a	g	-	-	-	-	-	-	-	a	t	t	t	t
<i>C. humicola</i> CMW 31183	t	a	c	c	t	c	t	a	g	-	-	-	-	-	-	-	a	t	t	t	t
<i>C. pseudospathiphylli</i> CBS 109165	-	a	c	c	a	c	c	a	g	c	t	c	c	g	a	-	-	a	a	t	t
<i>C. spathiphylli</i> CBS 114540	-	a	c	c	c	c	a	g	c	t	c	c	g	a	-	-	a	t	t	t	t

[†] Only polymorphic nucleotides occurring in all the isolates are shown, not alleles that partially occur in individuals per phylogenetic group. [‡] Numerical positions of the nucleotides in the DNA sequence alignments.

Phylogenetic analyses of the individual gene regions of *act*, *cmdA*, *his3*, *rpb2*, and *tub2* showed that the four isolates that resided in the CCSC were clustered in an independent clade (Suppl. material 1: Figs S1–S4, S6). However, the phylogenetic tree based on *tef1* showed that three of those isolates formed an independent clade, while one isolate was closely related to *C. metrosideri*, *C. pseudometrosideri*, and *C. candelabrum* (Suppl. material 1: Fig. S5). Based on the concatenated dataset of the six genes, the four isolates formed a new, strongly defined phylogenetic clade that was distinct from other *Calonectria* species in the CSSC and was supported by high bootstrap values (MP = 91%, ML = 99%) and high values of posterior probability (1.0) (Fig. 1). The four isolates of the new phylogenetic clade were distinguished from their phylogenetically closely related *Calonectria* species using SNP analyses for the six-gene concatenated dataset, by presenting eight unique SNPs from a total of 78 SNPs (Table 3). The results of these phylogenetic and SNP analyses indicate that the four isolates in the CCSC represent a distinct, undescribed species, which we named *C. imperata*.

Table 3. Single nucleotide polymorphisms found in *Calonectria imperata* and its phylogenetically closely related species in the six gene regions.

Species	<i>act</i> [†]										<i>cmdA</i>										<i>bis3</i>									
	57 [‡]	62	71	121	171	187	210	319	376	403	405	418	444	8	44	46	53	56	60	66										
<i>C. imperata</i> CCDCA 11649	c	a	c	c	g	g	c	c	t	t	c	t	t	c	c	t	c	g	a											
<i>C. brassiana</i> CBS 134855	c	gg	t	gg	gg	c	c	c	c	a	t	t	c	t	c	c	g	a												
<i>C. glaebicola</i> CBS 134852	a	c	c	gg	gg	c	gg	t	c	c	a	t	c	t	c	c	g	a												
<i>C. piauiensis</i> CBS 134850	a	gg	c	c	a	c	c	c	c	a	c	c	c	-	a	c	a	c												
<i>C. venezuelana</i> CBS 111052	t	a	c	c	g	gg	a	gg	t	c	t	a	t	c	c	t	g	a												
Species																					<i>bis3</i>									
	93	99	105	114	156	189	234	235	238	244	245	250	251	252	254	255	257	262	275	276										
<i>C. imperata</i> CCDCA 11649	c	c	c	a	t	t	t	c	c	a	c	c	a	gg	c	a	a	t	gg											
<i>C. brassiana</i> CBS 134855	c	c	c	t	t	t	t	c	c	a	c	c	a	gg	c	a	a	t	gg											
<i>C. glaebicola</i> CBS 134852	c	c	c	a	t	t	t	c	a	a	c	c	a	gg	c	a	a	t	gg											
<i>C. piauiensis</i> CBS 134850	t	t	c	a	c	t	c	g	t	g	g	t	a	gg	a	t	gg	g	c											
<i>C. venezuelana</i> CBS 111052	c	c	a	a	t	c	t	t	c	c	a	c	c	ag	c	a	a	t	gg											
Species	<i>bis3</i>										<i>rpb2</i>										<i>tef1</i>									
	277	278	333	336	351	405	420	105	603	624	693	840	47	81	110	112	135	220	239	357										
<i>C. imperata</i> CCDCA 11649	c	t	t	c	gg	c	t	gg	a	c	t	a	c	gg	a	t	t	c	c	c										
<i>C. brassiana</i> CBS 134855	c	t	t	c	gg	t	t						c	gg	t	t	c	c	c											
<i>C. glaebicola</i> CBS 134852	c	t	t	c	a	c	t						c	a	a	t	t	c	c											
<i>C. piauiensis</i> CBS 134850	t	t	c	t	g	c	g						t	gg	a	a	c	t	c											
<i>C. venezuelana</i> CBS 111052	c	c	t	c	g	c	t	t	g	t	c	gg	a	t	t	c	c	t												
Species	<i>tef1a</i>										<i>tub2</i>																			
	417	421	422	425	453	50	99	120	132	174	175	188	191	220	377	398	408	409												
<i>C. imperata</i> CCDCA 11649	c	c	c	a	a	c	a	g	t	c	c	gg	c	t	t	t	-	-												
<i>C. brassiana</i> CBS 134855	c	t	t	a	a	c	a	gg	t	c	c	gg	c	t	t	t	a	c												
<i>C. glaebicola</i> CBS 134852	c	t	t	a	a	c	a	gg	t	c	c	gg	c	t	t	t	a	c												
<i>C. piauiensis</i> CBS 134850	t	c	c	a	a	g	g	a	c	t	t	a	a	c	c	g	a	c												
<i>C. venezuelana</i> CBS 111052	c	c	c	c	g	c	a	g	t	c	c	g	c	t	t	t	a	c												

[†] Only polymorphic nucleotides occurring in all the isolates are shown, not alleles that partially occur in individuals per phylogenetic group. [‡] Numerical positions of the nucleotides in the DNA sequence alignments.

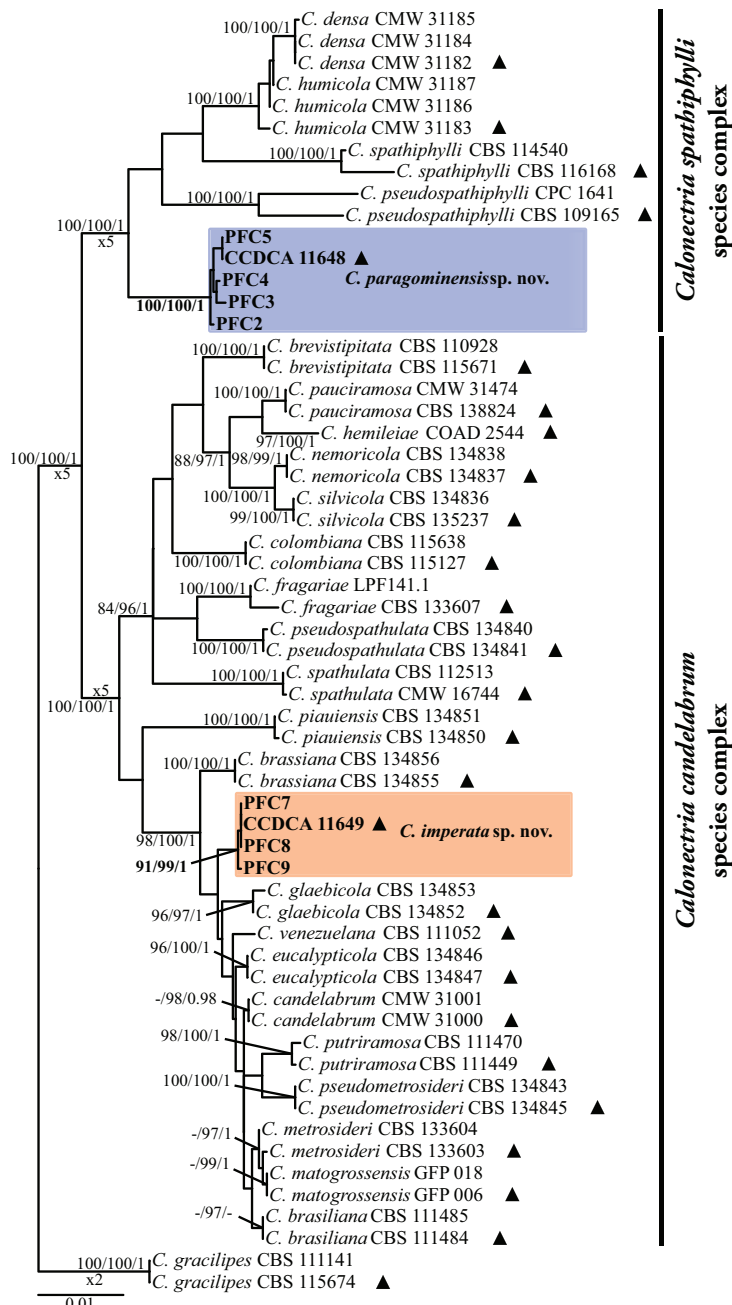


Figure 1. Phylogenetic tree based on maximum likelihood analysis of concatenated *act*, *cmdA*, *his3*, *rpb2*, *tef1* and *tub2* gene regions. Bootstrap support values $\geq 80\%$ for maximum parsimony (MP), Ultrafast bootstrap support values $\geq 95\%$ for maximum likelihood (ML), and posterior probability (PP) values ≥ 0.95 from BI analyses are presented at the nodes (MP/ML/PP). Bootstrap values below 80% (MP), 95% (ML) and posterior probabilities below 0.80 are marked with “-”. Ex-type isolates are indicated by “▲”, isolates highlighted in bold were sequenced in this study, and novel species are in blue and orange. *C. gracilipes* was used as outgroup. The scale bar indicates the number of nucleotide substitutions per site.

Species delimitation by GCPSR analysis

A PHI test using a five-locus concatenated dataset (*act*, *cmdA*, *his3*, *tef1*, *tub2*) was performed to determine the recombination level among *C. paragominensis* and its phylogenetically closely related species, *C. densa*, *C. humicola*, *C. spathiphylli* and *C. pseudospathiphylli*. A value of $\Phi_w = 0.2879$ revealed no significant genetic recombination events, and this relationship was supported with a high bootstrap value (100%) in the phylogenetic network analysis, indicating that they are different species (Fig. 2A).

A PHI test using a four-locus concatenated dataset (*cmdA*, *his3*, *tef1*, *tub2*) was performed to determine the recombination level among *C. imperata* and its

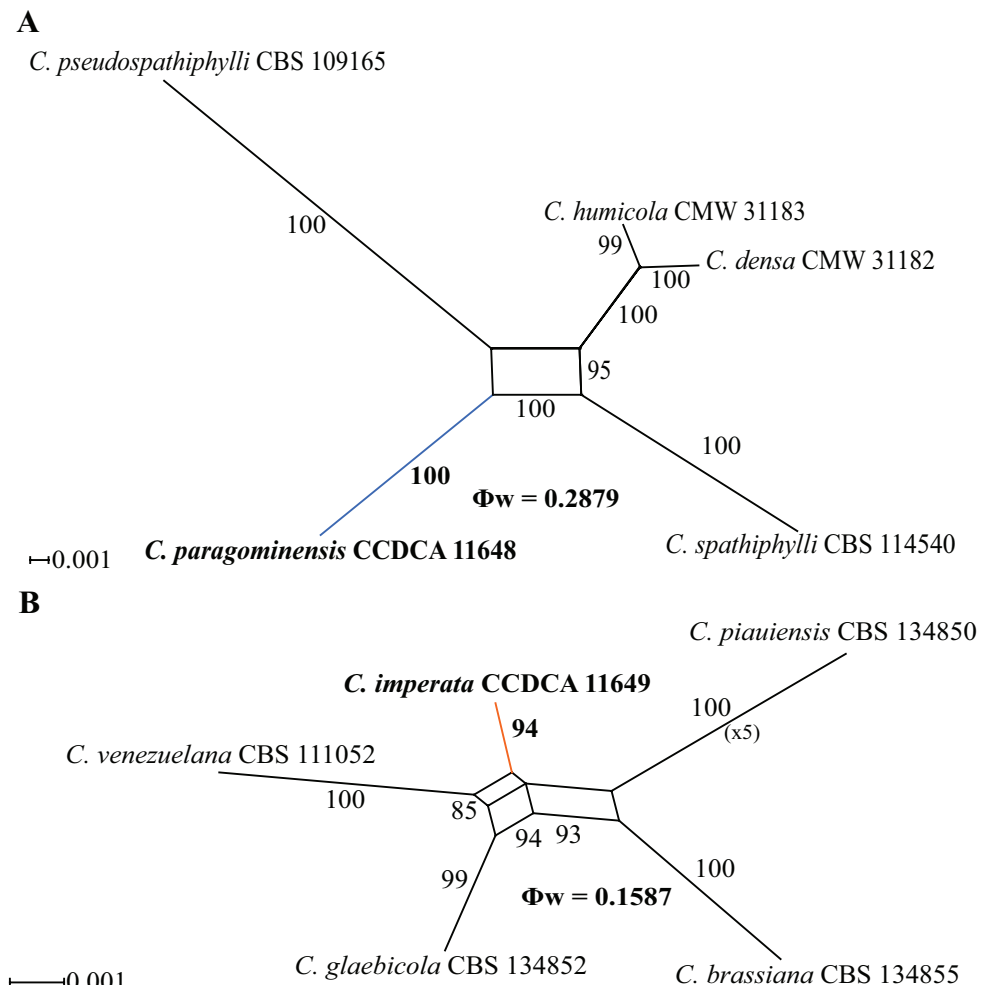


Figure 2. Results of the pairwise homoplasy index (PHI) test for *C. paragominensis* and *C. imperata*. Phylogenetic networks constructed using the LogDet transformation and the NeighborNet method and displayed with the EqualAngle algorithm. Bootstrap support values > 80% are shown. $\Phi_w < 0.05$ indicate significant recombination. New species described in this study are highlighted in bold, with blue (**A**) and orange (**B**) lines.

phylogenetically closely related species, *C. brassiana*, *C. glabeicola*, *C. piauiensis*, and *C. venezuelana*. A value of $\Phi_W = 0.1587$ revealed no significant genetic recombination events, and this relationship was supported with a high bootstrap value (94%) in the phylogenetic network analysis, indicating that they are different species (Fig. 2B).

Mating-type and sexual compatibility test

MAT1-1-1 and MAT1-2-1 genes were amplified in all isolates of each identified species, indicating that they are putatively homothallic. However, after a twelve-week mating test on MSA, all isolates failed to yield sexual structures, indicating that they have lost the ability to be self-fertile or have retained the ability to favor outcrossing rather than selfing.

Taxonomy

Based on phylogenetic analyses, GCPSR, and network analyses, the nine isolates presented two strongly defined phylogenetic clades in both the *Calonectria spathiphylli* species complex and the *Calonectria candelabrum* species complex. Morphological differences, especially in the macroconidia and stipe dimensions, were observed between each phylogenetic clade and its phylogenetically closely related species (Table 4). Thus, the fungi isolated in this study represent two new species of *Calonectria* and are described as follows:

Calonectria paragominensis E.I.Sánchez, T.P.F.Soares & M.A.Ferreira, sp. nov.

MycoBank No: 843460

Fig. 3

Etymology. The term “*paragominensis*” refers to the microregion of Paragominas, Brazil, which is the place where the fungus was collected.

Diagnosis. *Calonectria paragominensis* differs from the phylogenetically closely related species *C. densa*, *C. humicola*, *C. spathiphylli* and *C. pseudospathiphylli* with respect to its macroconidia dimensions.

Type. BRAZIL, Pará state, Paragominas microregion; 3°10'51"S, 47°18'49"W; From infected leaves of *E. grandis* × *E. brassiana*; 20 Feb. 2020; M.A. Ferreira; **holotype:** UB24349, **ex-type:** CCDCA 11648 = PFC1. GenBank: *act* = ON009346; *cmdA* = OM974325; *his3* = OM974334; *rpb2* = OM974343; *tef1* = OM974352; *tub2* = OM974361.

Description. Sexual morph unknown. Macroconidiophores consisted of a stipe, a suite of penicillate arrangements of fertile branches, a stipe extension, and a terminal vesicle; stipe septate, hyaline, smooth, (112–)135–207(–281) × (2–)2.6–3.5(–4) µm; stipe extension septate, straight to flexuous, (123–)147–220(–295) µm long, (1.5–)1.9–2.4(–3) µm wide at the apical septum, terminating in a globose to

Table 4. Morphological characteristics of two new *Calonectria* species and their phylogenetically closely related species.

Species complex	Species	Conidiogenus apparatus	Spike	Extension	Macroconidia	Vesicle	Shape	Reference
		Size (L × W) ^{†‡§}	Branches	Size (L × W) ^{†‡§}	Size (L × W) ^{†‡§}	Average Septa Diameter ^{†‡§}	(L × W) ^{†‡§}	
<i>Calonectria spathiphylli</i> species complex								
<i>C. paragominensis</i>	40–113 × 45–129	(–4)	112–281 × 2–4	123–295 × 1.5–3	(47–)56–66(–71) × (4–)4.8–5.9(–7)	61 × 5	1(–3)	8–12 globoid to sphaeropedunculate
<i>C. densa</i>	49–78 × 63–123	(–4)	54–90 × 6–10	149–192 × 5–6	(47–)50–58(–62) × (5–)6	54 × 6	1	10–12 ovoid to ellipsoid to sphaeropedunculate
<i>C. humicola</i>	43–71 × 42–49	3	44–90 × 6–8	126–157 × 4–5	(45–)48–54(–56) × (4–)5	51 × 5	1	10–12 globose to ovoid to sphaeropedunculate
<i>C. pseudospathiphylli</i>	70–100 × 25–70	4	100–350 × 5–6	100–250 × 2.5–3.5	(40–)47–55(–60) × 4–5	52 × 4	1(–3)	8–12 sphaeropedunculate to ellipsoid
<i>C. spathiphylli</i>	60–150 × 40–90	4	120–150 × 6–8	170–260 × 3–4	(45–)65–80(–120) × (5–)6(–7)*	70 × 6	1(–3)	8–15 globose or ellipsoid to obpyriform
<i>Calonectria canelabrum</i> species complex								
<i>C. imperata</i>	50–127 × 41–110	(–3)	135–227 × 2–4	151–254 × 1.5–3	(38–)43–49(–52) × (2–)2.7–3.2(–4)	46 × 3	(–1)	3–6 ellipsoid to narrowly obpyriform
<i>C. piatensis</i>	20–60 × 35–80	2	50–110 × 4–6	95–130 × 2–3	(38–)47–52(–60) × 3–5	49 × 4.5	1	3–7 ellipsoid to narrowly obpyriform
<i>C. brasiliensis</i>	50–80 × 50–135	3	55–155 × 5–8	90–172 × 2–3	(35–)50–56(–65) × 3–5	53 × 4	1	3–7 ellipsoid to narrowly obpyriform
<i>C. glabricula</i>	27–45 × 25–40	2	50–130 × 5–7	100–165 × 2–4	(45–)50–52(–55) × 3–5	50 × 4	1	3–5 ellipsoid to narrowly obpyriform
<i>C. venezuelana</i>	25–65 × 25–60	3	35–100 × 4–8	85–190 × 3–6	(48–)54–62(–65) × (4–)4.5–5.5(–7)	58 × 5	1	5–9 fusiform to ovoid to ellipsoid

† All measurements are in µm. ‡ L × W = length × width. § Minimum–maximum. | Measurements are presented in the format [minimum–] (average – standard deviation) – (average + standard deviation) (– maximum)]. ¶ Measurements are presented in the format [(minimum–) (average) (–maximum)].

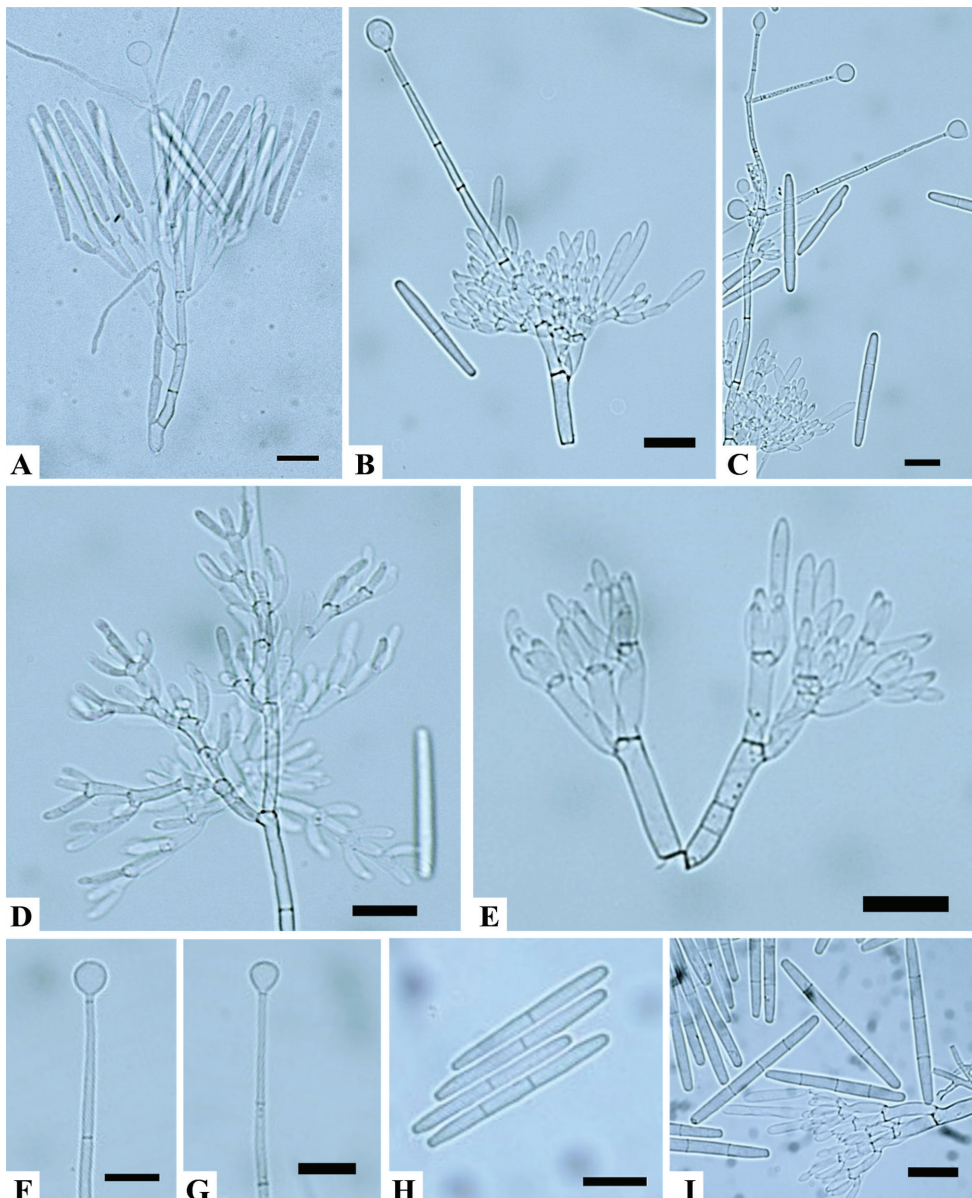


Figure 3. *Calonectria paragominensis* **A, B** macroconidiophore **C** lateral stipe extensions **D, E** conidiogenous apparatus with conidiophore branches and doliiform to reniform phialides **F, G** globose to sphaeropedunculate vesicles **H, I** one, two, and three-septate macroconidia. Scale bars: 20 μm .

sphaeropedunculate vesicle, (8–)8.5–10.5(–12) μm diam; lateral stipe extensions (90° to the axis) also present. Conidiogenous apparatus was (40–)56–88(–113) μm long, (45–)67–107(–129) μm wide; primary branches aseptate or 1-septate, (15.7–)18.4–25.9(–30.6) \times (3.3–)4–6(–6.5) μm ; secondary branches aseptate, (12.7–)14.3–

19.6(–22.1) × (3–)3.5–5(–6) µm; tertiary branches aseptate, (9.9–)11.6–15.3(–17.9) × (2.8–)3.6–5.3(–6.4) µm; additional branches (–4), aseptate, (10.3–)11–13.2(–14) × (3–)3.2–4.4(–5) µm; each terminal branch produced 2–4 phialides; phialides doliform to reniform, hyaline, aseptate, (8–)9.1–11.8(–14) × (2–)2.7–4.1(–6) µm, apex with minute periclinal thickening and inconspicuous collarette. Macroconidia were cylindrical, rounded at both ends, straight, (47–)56–66(–71) × (4–)4.8–5.9(–7) µm (av. = 61 × 5 µm), (1–3) septate, lacking a visible abscission scar, held in parallel cylindrical clusters by colorless slime. Megaconidia and microconidia were not observed.

Culture characteristics. Colonies formed abundant white aerial mycelium on MEA at 25 °C after seven days, with irregular margins and moderate sporulation. The surface had white to buff outer margins, and sienna to amber in reverse with abundant chlamydospores throughout the medium, forming microsclerotia. The optimal growth temperature was 23.8 °C, with no growth at 5 °C; after seven days, colonies at 10 °C, 15 °C, 20 °C, 25 °C, and 30 °C reached 7 mm, 23 mm, 38.3 mm, 36.1 mm, and 31.8 mm, respectively.

Substratum. Leaves of *E. grandis* × *E. brasiliensis*.

Distribution. Northeast Brazil.

Other specimens examined. BRAZIL,• Pará state, Paragominas microregion; From infected leaves of *E. grandis* × *E. brasiliensis*; 20 Feb. 2020; M.A. Ferreira; cultures PFC2, PFC3, PFC4, PFC5.

Notes. *C. paragominensis* is a new species in the *C. spathiphylli* species complex (Liu et al., 2020). Morphologically, *C. paragominensis* is very similar to *C. densa*, since both form lateral stipe extensions, which have not been reported for the other three species in the complex. However, the macroconidia of *C. paragominensis* (av. 61 × 5 µm) are longer than those of *C. densa* (av. 54 × 6 µm), *C. humicola* (av. 51 × 5 µm) and *C. pseudospathiphylli* (av. 52 × 4 µm) but smaller than those of *C. spathiphylli* (av. 70 × 6 µm).

Calonectria imperata E.I.Sánchez, T.P.F.Soares & M.A.Ferreira, sp. nov.

MycoBank No: 843461

Fig. 4

Etymology. The term “*imperata*” is in honor of the city of Imperatriz, Brazil, which was close to the place where the fungus was collected.

Diagnosis. *Calonectria imperata* differs from the phylogenetically closely related species *C. brasiliensis*, *C. glaebicola*, *C. piauiensis* and *C. venezuelana* with respect to the number of unique alleles and stipe dimensions.

Type. BRAZIL,• Maranhão state, Cidelândia municipality; 5°09'24"S, 47°46'26"W; From infected leaves of *E. urophylla*; 20 Feb. 2020; M.A. Ferreira; **holotype:** UB24350, **ex-type:** CCDCA 11649 = PFC6. GenBank: *act* = ON009351; *cmdA* = OM974330; *his3* = OM974339; *rpb2* = OM974348; *tef1* = OM974357; *tub2* = OM974366.

Description. Sexual morph unknown. Macroconidiophores consisted of a stipe, a suite of penicillate arrangements of fertile branches, a stipe extension, and a terminal vesicle; stipe septate, hyaline, smooth, (135–)151–198(–227) × (2–)2.6–3.4(–4) µm; stipe extension

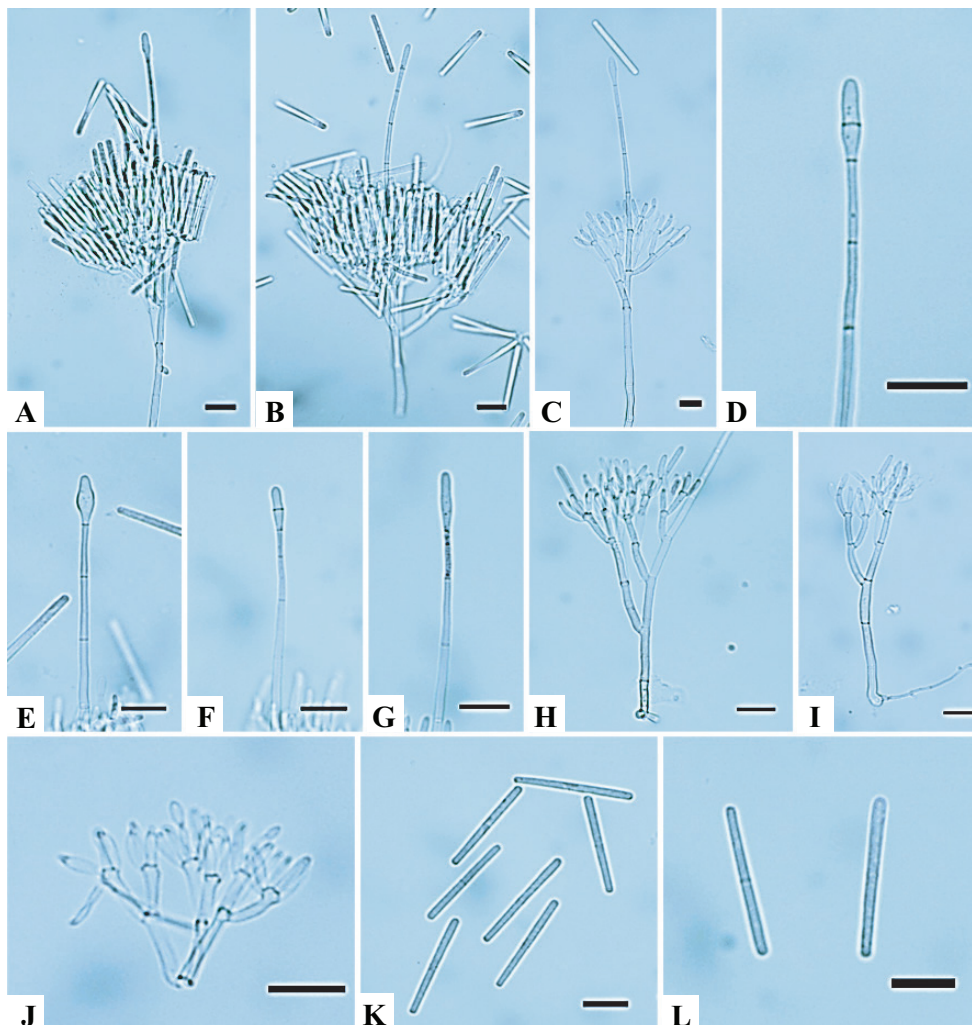


Figure 4. *Calonectria imperata* **A–C** macroconidiophore **D–G** ellipsoidal to narrowly obpyriform vesicles **H–J** conidiogenous apparatus with conidiophore branches and doliiiform to reniform phialides **K, L** macroconidia. Scale bars: 20 μm .

septate, straight to flexuous, (151–)169–220(–254) μm long, (1.5–)1.9–2.7(–3) μm wide at the apical septum, terminating in an ellipsoidal to narrowly obpyriform vesicle (3–)3.1–4.6(–6) μm diam. Conidiogenous apparatus was (50–)66–100(–127) μm long, (41–)62–89(–110) μm wide; primary branches aseptate, (14.6–)19–24.8(–28.5) \times (2.5–)3.2–4(–4.5) μm ; secondary branches aseptate, (12.1–)13.5–18.2(–24.2) \times (2.3–)2.8–3.7(–4) μm ; tertiary branches aseptate, (10.1–)11–15(–18.1) \times (1.9–)2.3–3.2(–4.1) μm ; each terminal branch producing 2–4 phialides; phialides doliiiform to reniform, hyaline, aseptate, (8–)9.1–13(–15) \times (2–)2.7–3.3(–4) μm , apex with minute periclinal thickening and inconspicuous collarette. Macroconidia were cylindrical, rounded at both ends,

straight, (38–)43–49(–52) × (2–)2.7–3.2(–4) µm (av. = 46 × 3 µm), (–1) septate, lacking a visible abscission scar, held in parallel cylindrical clusters by colorless slime. Megaconidia and microconidia were not observed.

Culture characteristics. Colonies formed moderate aerial mycelium on MEA at 25 °C after seven days, with moderate sporulation. The surface had white to buff outer margins, and sepia to umber in reverse with abundant chlamydospores throughout the medium, forming microsclerotia. The optimal growth temperature was 25 °C, with no growth at 5 °C; after seven days, colonies at 10 °C, 15 °C, 20 °C, 25 °C, and 30 °C reached 10.1 mm, 25.5 mm, 29.1 mm, 44.5 mm, and 40.6 mm, respectively.

Substratum. Leaves of *E. urophylla*.

Distribution. Northeast Brazil.

Other specimens examined. BRAZIL• Maranhão state, Cidelândia municipality; 5°09'24"S, 47°46'26"W; From infected leaves of *E. urophylla*; 20 Feb. 2020; M.A. Ferreira; cultures PFC7, PFC8, PFC9. BRAZIL• Maranhão state, Itinga do Maranhão; 4°34'43"S, 47°29'48"W; from infected leaves of *E. urophylla*; 20 Feb. 2020; M.A. Ferreira; culture PFC9.

Notes. *C. imperata* is a new species in the *C. candelabrum* species complex (Liu et al., 2020). Morphologically, *C. imperata* is very similar to its closest relatives, from which it can be distinguished based on stipe dimensions and phylogenetic inference. Stipe of *C. imperata* (135–227 × 2–4 µm) is larger than those of *C. piauiensis* (50–110 × 4–6 µm), *C. glaebicola* (50–130 × 5–7 µm), and *C. venezuelana* (35–100 × 4–8 µm) but narrower than those of *C. brassiana* (55–155 × 5–8 µm). Additionally, *C. imperata* lacks lateral stipe extensions, which are present in *C. piauiensis*.

Pathogenicity tests

The conidia suspensions of the representative isolates of *C. paragominensis* and *C. imperata* produced lesion symptoms on leaves (Fig. 5E, F, I, J), but no lesions were observed on the negative control inoculations (Fig. 5G, H, K). The pathogens were reisolated from inoculated leaves but not from the negative controls and identified by the same morphological characteristics as the originally inoculated species, thus, fulfilling the requirements of Koch's postulates.

Discussion

Two new species of *Calonectria* isolated from diseased *Eucalyptus* leaves were identified based on phylogenetic analyses of six gene regions and on morphological comparisons. These two species were named *C. paragominensis* and *C. imperata*.

Calonectria paragominensis is a new species in the *C. spathiphylli* complex. The five species identified and described in *C. spathiphylli* complex are *C. densa*, *C. humicola*, *C. spathiphylli*, *C. pseudospathiphylli*, and *C. paragominensis*, where *C. paragominensis* can be differentiated morphologically with respect to the macroconidia dimensions

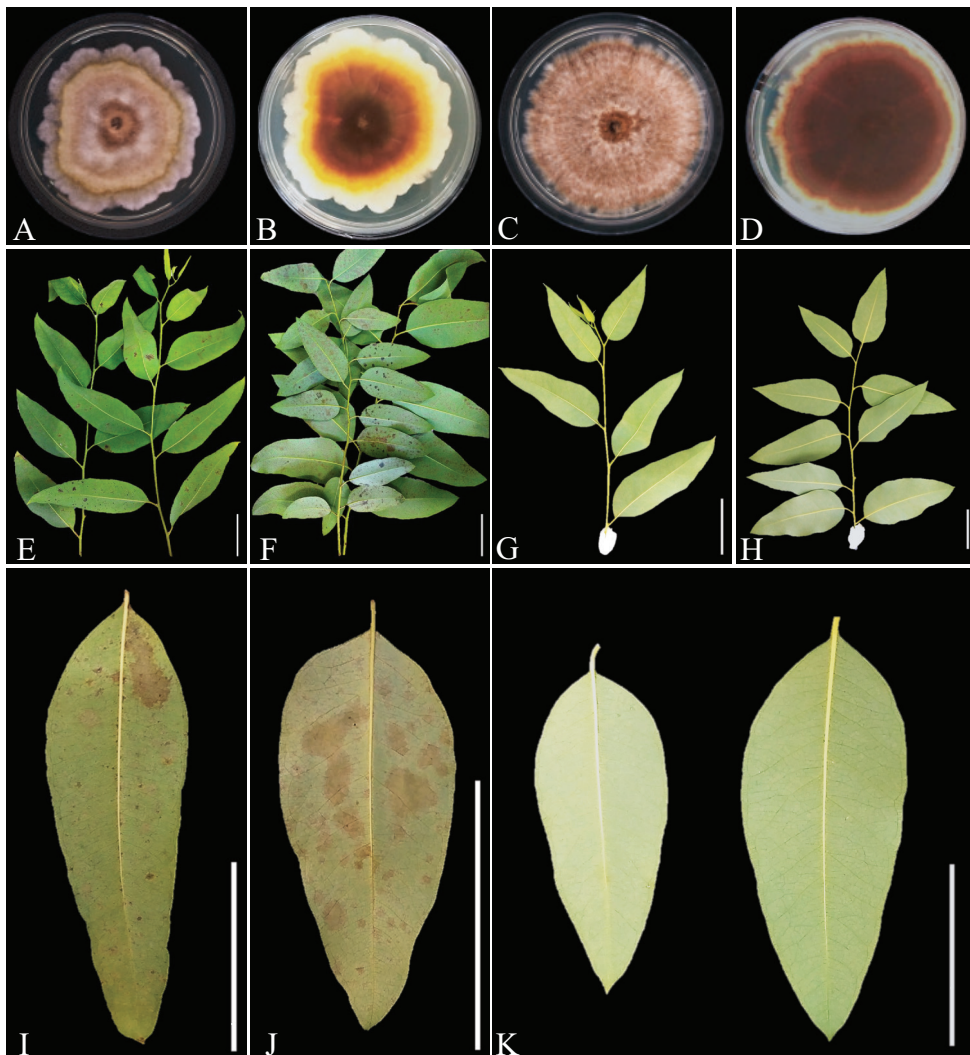


Figure 5. Pathogenicity tests on leaves of *Eucalyptus* genotypes **A, B** surface and reverse of *C. paragominensis* on MEA plates after 14 days grown at 25 °C **C, D** surface and reverse of *C. imperata* on MEA plates after 14 days grown at 25 °C **E, I** lesions on leaves of *E. grandis* × *E. brassiana* induced by *C. paragominensis* 72 h after inoculation **F, J** lesions on leaves of *E. urophylla* induced by *C. imperata* 72 h after inoculation **G, H, K** no disease symptoms on leaves inoculated with sterile water (negative controls). Scale bars: 5 cm (**E–K**).

(El-Gholl et al. 1992; Kang et al. 2001; Crous 2002; Lombard et al. 2010b). These species are characterized by presenting globoid to ovoid to sphaeropedunculate terminal vesicles (Kang et al. 2001; Crous 2002; Lombard et al. 2010b). *Calonectria spathiphylli* is described as heterothallic (El-Gholl et al. 1992), *C. densa* as putatively heterothallic (Li et al. 2020) and *C. pseudospatiphilly* as homothallic (Kang et al. 2001). The *C. humicola* mating type has not been indicated (Lombard et al. 2010b). Here,

C. paragominensis is described as putatively homothallic based on PCR amplification of the mating-type genes. Regarding pathogenicity, *C. paragominensis* is pathogenic to *Eucalyptus* sp., *C. spathiphylli* is pathogenic to *Sapthiphyllum* sp. *Heliconia* sp. *Ludwigia* sp. *Strelitzia* sp. and *Eugenia* sp. (El-Gholl et al. 1992; Poltronieri et al. 2011). *Calonectria densa*, *C. humicola*, and *C. pesudospathiphylli* were isolated from soil, and their pathogenicity has not been indicated (Kang et al. 2001; Lombard et al. 2010b). In addition to *C. paragominensis*, only *C. spathiphylli* has been indicated to be present in Brazil (Reis et al. 2004; Poltronieri et al. 2011).

Calonectria imperata is a new species in the *C. candelabrum* complex. Species in this complex are characterized by presenting ellipsoidal to obpyriform terminal vesicles, in both heterothallic and homothallic species, and occur in Africa, Asia, Europe, North and South America, and Oceania (Liu et al. 2020). Of the 21 species in the *C. candelabrum* complex (Crous et al. 2018, 2019; Liu et al. 2020), 17 have been found in Brazil (Schoch et al. 1999; Crous et al. 2018, 2019; Liu et al. 2020). *Calonectria imperata* is phylogenetically closely related to *C. brassiana*, *C. glaebicola*, *C. piauiensis* and *C. venezuelana*, which can be differentiated with respect to the number of unique alleles and stipe dimensions (Alfenas et al. 2015; Lombard et al. 2016). *Calonectria brassiana*, *C. glaebicola*, and *C. piauiensis* were found in Brazil, isolated from soil samples of *Eucalyptus* plantations, but only *C. glaebicola* has been confirmed to be pathogenic to *Eucalyptus* sp. (Alfenas et al. 2015). *Calonectria venezuelana* was reported in Venezuela, similarly, isolated from soil samples, but its pathogenicity has not been indicated (Lombard et al. 2016). The mating-type for *C. brassiana*, *C. glaebicola*, *C. piauiensis* and *C. venezuelana* has not been determined (Liu et al. 2020).

Pathogenicity tests showed that *C. paragominensis* and *C. imperata* are pathogenic to *E. grandis* × *E. brassiana* hybrid genotype and *E. urophylla* genotype, respectively. Although the death of *Eucalyptus* trees due to CLB is not common, it affects *Eucalyptus* plants most severely from six months to 2–3 years after planting (Graça et al. 2009). Although the economic loss due to defoliation caused by CLB has not been quantified directly, according to artificial pruning studies conducted by Pulrolnik et al. (2005) and Pires (2000), when the loss of branches is equal to or greater than 75% of *E. grandis* seedlings of one year of age, the volumetric productivity has decreased by 45% by the time they reach seven years old. Therefore, it has been inferred that in susceptible clones, the pathogen can cause economic losses, since under favorable conditions, infection by *Calonectria* can result in severe defoliation (Soares et al. 2018). Additionally, Miranda et al. (2021) indicated a potential growth loss of 19.8 to 39.6% due to CLB, and by using the estimates of growth reduction from Pires (2000) as a baseline, concluded that a reduction in the volumetric increment to the order of 39.6% may result in an economic loss of R\$ 4291.00 per ha, considering a price of *Eucalyptus* wood as R\$ 38.70 per m³ (IEA 2020) and a production of 280 m³.ha⁻¹ in the first 7-year rotation. Therefore, accurate diagnoses of plant diseases and identification of their causal agents are fundamental in promoting the development of effective disease management strategies (Wingfield et al. 2015; Liu and Chen 2017).

In this study, we described two new *Calonectria* species, both isolated from diseased *Eucalyptus* leaves from commercial plantations localized in a tropical zone. These results suggest that there are still more *Calonectria* species to be discovered in Brazil, and that they require careful monitoring, since this knowledge could facilitate the development of resistant *Eucalyptus* clones.

Acknowledgements

We thank Heitor S. Dallapiccola and Francisco J. A. Gomes for their help during sample collection. We thank the laboratories of Molecular Biology, Plant Virology, and Nematology at Universidade Federal de Lavras (UFLA) for the facilities granted during the completion of this study. The first author thanks the “Coordenação de Aperfeiçoamento de Pessoal de Nível Superior (CAPES)” for the doctorate scholarship assigned through Brazil’s PAEC OAS-GCUB Scholarships Program.

References

- Alfenas AC, Zauza EAV, Mafia RG, de Assis TF (2009) Clonagem e doenças do eucalipto. 2nd ed., Editora UFV, Viçosa, MG, Brazil, 500 pp.
- Alfenas RF, Pereira OL, Freitas RG, Freitas CS, Dita MA, Alfenas AC (2013) Mass spore production and inoculation of *Calonectria pteridis* on *Eucalyptus* spp. under different environmental conditions. Tropical Plant Pathology 38(5): 406–413. <https://doi.org/10.1590/S1982-56762013000500005>
- Alfenas RF, Lombard L, Pereira OL, Alfenas AC, Crous PW (2015) Diversity and potential impact of *Calonectria* species in *Eucalyptus* plantations in Brazil. Studies in Mycology 80(1): 89–130. <https://doi.org/10.1016/j.simyco.2014.11.002>
- Bruen TC, Philippe H, Bryant D (2006) A simple and robust statistical test for detecting the presence of recombination. Genetics 172(4): 2665–2681. <https://doi.org/10.1534/genetics.105.048975>
- Carbone I, Kohn LM (1999) A method for designing primer sets for speciation studies in filamentous ascomycetes. Mycologia 91(3): 553–556. <https://doi.org/10.1080/00275514.1999.12061051>
- Castellani A (1939) Viability of some pathogenic fungi in distilled water. The Journal of Tropical Medicine and Hygiene 42: 225–226.
- Chernomor O, Von Haeseler A, Minh BQ (2016) Terrace aware data structure for phylogenomic inference from supermatrices. Systematic Biology 65(6): 997–1008. <https://doi.org/10.1093/sysbio/syw037>
- Crous PW (2002) Taxonomy and pathology of *Cylindrocladium* (*Calonectria*) and allied genera. APS Press, St. Paul, Minnesota, USA, 278 pp.
- Crous PW, Groenewald JZ, Risède JM, Simoneau P, Hywel-Jones NL (2004) *Calonectria* species and their *Cylindrocladium* anamorphs: Species with sphaeropedunculate vesicles. Studies in Mycology 50: 415–430. <https://doi.org/10.3114/sim.55.1.213>

Crous PW, Luangsa-ard JJ, Wingfield MJ, Carnegie AJ, Hernández-Restrepo M, Lombard L, Roux J, Barreto RW, Baseia IG, Cano-Lira JF, Martín MP, Morozova OV, Stchigel AM, Summerell BA, Brandrud TE, Dima B, García D, Giraldo A, Guarro J, Gusmão LFP, Khamsuntorn P, Noordeloos ME, Nuankaew S, Pinruan U, Rodríguez-Andrade E, Souza-Motta CM, Thangavel R, van Iperen AL, Abreu VP, Accioly T, Alves JL, Andrade JP, Bahram M, Baral H-O, Barbier E, Barnes CW, Bendiksen E, Bernard E, Bezerra JDP, Bezerra JL, Bizio E, Blair JE, Bulyonkova TM, Cabral TS, Caiafa MV, Cantillo T, Colmán AA, Conceição LB, Cruz S, Cunha AOB, Darveaux BA, da Silva AL, da Silva GA, da Silva GM, da Silva RMF, de Oliveira RJV, Oliveira RL, De Souza JT, Dueñas M, Evans HC, Epifani F, Felipe MTC, Fernández-López J, Ferreira BW, Figueiredo CN, Filippova NV, Flores JA, Gené J, Ghorbani G, Gibertoni TB, Glushakova AM, Healy R, Huhndorf SM, Iturrieta-González I, Javan-Nikkhah M, Juciano RF, Jurjević Ž, Kachalkin AV, Keochanpheng K, Krisai-Greilhuber I, Li Y-C, Lima AA, Machado AR, Madrid H, Magalhães OMC, Marbach PAS, Melanda GCS, Miller AN, Mongkolsamrit S, Nascimento RP, Oliveira TGL, Ordoñez ME, Orzes R, Palma MA, Pearce CJ, Pereira OL, Perrone G, Peterson SW, Pham THG, Piontelli E, Pordel A, Quijada L, Raja HA, Rosas de Paz E, Ryvarden L, Saitta A, Salcedo SS, Sandoval-Denis M, Santos TAB, Seifert KA, Silva BDB, Smith ME, Soares AM, Sommai S, Sousa JO, Suetrong S, Susca A, Tedersoo L, Telleria MT, Thanakitipattana D, Valenzuela-Lopez N, Visagie CM, Zapata M, Groenewald JZ (2018) Fungal Plant description sheets: 785–867. Persoonia: Molecular Phylogeny and Evolution of Fungi 41(1): 238–417. <https://doi.org/10.3767/persoonia.2018.41.12>

Crous PW, Carnegie AJ, Wingfield MJ, Sharma R, Mughini G, Noordeloos ME, Santini A, Shouche YS, Bezerra JDP, Dima B, Guarnaccia V, Imrefi I, Jurjević Ž, Knapp DG, Kovács GM, Magistà D, Perrone G, Rämä T, Rebriev YA, Shivas RG, Singh SM, Souza-Motta CM, Thangavel R, Adhavure NN, Alexandrova AV, Alfenas AC, Alfenas RF, Alvarado P, Alves AL, Andrade DA, Andrade JP, Barbosa RN, Barili A, Barnes CW, Baseia IG, Bel-langer J-M, Berlanas C, Bessette AE, Bessette AR, Biketova AYU, Bomfim FS, Brandrud TE, Bransgrove K, Brito ACQ, Cano-Lira JF, Cantillo T, Cavalcanti AD, Cheewangkoon R, Chikowski RS, Conforto C, Cordeiro TRL, Craine JD, Cruz R, Damm U, de Oliveira RJV, de Souza JT, de Souza HG, Dearnaley JDW, Dimitrov RA, Dovana F, Erhard A, Esteve-Raventós F, Félix CR, Ferisin G, Fernandes RA, Ferreira RJ, Ferro LO, Figueiredo CN, Frank JL, Freire KTLS, García D, Gené J, Gęsiorska A, Gibertoni TB, Gondra RAG, Gouliamova DE, Gramaje D, Guard F, Gusmão LFP, Haitook S, Hirooka Y, Houbraken J, Hubka V, Inamdar A, Iturriaga T, Iturrieta-González I, Jadon M, Jiang N, Justo A, Kacha-lkin AV, Kapitonov VI, Karadelev M, Karakehian J, Kasuya T, Kautmanová I, Kruse J, Kušan I, Kuznetsova TA, Landell MF, Larsson K-H, Lee HB, Lima DX, Lira CRS, Macha-do AR, Madrid H, Magalhães OMC, Majerova H, Malysheva EF, Mapperson RR, Marbach PAS, Martín MP, Martín-Sanz A, Matočec N, McTaggart AR, Mello JF, Melo RFR, Mešić A, Michereff SJ, Miller AN, Minoshima A, Molinero-Ruiz L, Morozova OV, Mosoh D, Nabe M, Naik R, Nara K, Nascimento SS, Neves RP, Olariaga I, Oliveira RL, Oliveira TGL, Ono T, Ordoñez ME, de M Ottoni A, Paiva LM, Pancorbo F, Pant B, Pawłowska J, Peterson SW, Raudabaugh DB, Rodríguez-Andrade E, Rubio E, Rusevska K, Santiago ALCMA, Santos ACS, Santos C, Sazanova NA, Shah S, Sharma J, Silva BDB, Siquier JL, Sonawane MS, Stchigel AM, Svetasheva T, Tamakeaw N, Telleria MT, Tiago PV, Tian

- CM, Tkalčec Z, Tomashevskaya MA, Truong HH, Vecherskii MV, Visagie CM, Vizzini A, Yilmaz N, Zmitrovich IV, Zvyagina EA, Boekhout T, Kehlet T, Læssøe T, Groenewald JZ (2019) Fungal Planet description sheets: 868–950. Persoonia: Molecular Phylogeny and Evolution of Fungi 42: 291–473. <https://doi.org/10.3767/persoonia.2019.42.11>
- Crous PW, Hernández-Restrepo M, Schumacher RK, Cowan DA, Maggs-Kölling G, Marais E, Wingfield MJ, Yilmaz N, Adan OCG, Akulov A, Duarte E, Berraf-Tebbal A, Bulgakov TS, Carnegie AJ, de Beer ZW, Decock C, Dijksterhuis J, Duong TA, Eichmeier A, Hien LT, Houbraken JAMP, Khanh TN, Liem NV, Lombard L, Lutzoni FM, Miadlikowska JM, Nel WJ, Pascoe IG, Roets F, Roux J, Samson RA, Shen M, Spetik M, Thangavel R, Thanh HM, Thao LD, van Nieuwenhuijzen EJ, Zhang JQ, Zhang Y, Zhao LL, Groenewald JZ (2021a) New and Interesting Fungi 4. Fungal Systematics and Evolution 7(1): 255–343. <https://doi.org/10.3114/fuse.2021.07.13>
- Crous PW, Cowan DA, Maggs-Kölling G, Yilmaz N, Thangavel R, Wingfield MJ, Noordeloos ME, Dima B, Brandrud TE, Jansen GM, Morozova OV, Vila J, Shivas RG, Tan YP, Bishop-Hurley S, Lacey E, Marney TS, Larsson E, Le Floch G, Lombard L, Node P, Hubka V, Alvarado P, Berraf-Tebbal A, Reyes JD, Delgado G, Eichmeier A, Jordal JB, Kachalkin AV, Kubátová A, Maciá-Vicente JG, Malysheva EF, Papp V, Rajeshkumar KC, Sharma A, Spetik M, Szabóová D, Tomashevskaya MA, Abad JA, Abad ZG, Alexandrova AV, Anand G, Arenas F, Ashtekar N, Balashov S, Bañares Á, Baroncelli R, Bera I, Biketova AYU, Blomquist CL, Boekhout T, Boertmann D, Bulyonkova TM, Burgess TI, Carnegie AJ, Cobo-Díaz JF, Corriol G, Cunningham JH, da Cruz MO, Damm U, Davoodian N, de A Santiago ALCM, Dearnaley J, de Freitas LWS, Dhileepan K, Dimitrov R, Di Piazza S, Fatima S, Fuljer F, Galera H, Ghosh A, Giraldo A, Glushakova AM, Gorczak M, Gouliamova DE, Gramaje D, Groenewald M, Gunsch CK, Gutiérrez A, Holdom D, Houbraken J, Ismailov AB, Istel Ł, Iturriaga T, Jeppson M, Jurjević Ž, Kalinina LB, Kapitonov VI, Kautanova I, Khalid AN, Kiran M, Kiss L, Kovács Á, Kurose D, Kusan I, Lad S, Læssøe T, Lee HB, Luangsa-ard JJ, Lynch M, Mahamed AE, Malysheva VF, Mateos A, Matočec N, Mešić A, Miller AN, Mongkolsamrit S, Moreno G, Morte A, Mostowfizadeh-Ghalamfarsa R, Naseer A, Navarro-Ródénas A, Nguyen TTT, Noisripoom W, Ntandu JE, Nuytinck J, Ostrý V, Pankratov TA, Pawłowska J, Pecenka J, Pham THG, Polhorský A, Posta A, Raudabaugh DB, Reschke K, Rodríguez A, Romero M, Rooney-Latham S, Roux J, Sandoval-Denis M, Smith MTh, Steinrücken TV, Svetasheva TY, Tkalčec Z, van der Linde EJ, vd Vegte M, Vauras J, Verbeken A, Visagie CM, Vitelli JS, Volobuev SV, Weill A, Wrzosek M, Zmitrovich IV, Zvyagina EA, Groenewald JZ (2021b) Fungal planet description sheets: 1182–1283. Persoonia: Molecular Phylogeny and Evolution of Fungi 46: 313–528. <https://doi.org/10.3767/persoonia.2021.46.11>
- Cunningham CW (1997) Can three incongruence tests predict when data should be combined? Molecular Biology and Evolution 14(7): 733–740. <https://doi.org/10.1093/oxfordjournals.molbev.a025813>
- Dress AW, Huson DH (2004) Constructing splits graphs. IEEE/ACM Transactions on Computational Biology and Bioinformatics 1(3): 109–115. <https://doi.org/10.1109/TCBB.2004.27>
- El-Gholl NE, Uchida JY, Alfenas AC, Schubert TS, Alfieri SA (1992) Induction and description of perithecia of *Calonectria spathiphylli* sp. nov. Mycotaxon 45: 285–300.

- Farris JS, Kallersjo M, Kluge AG, Bult C (1995) Testing significance of incongruence. *Cladistics* 10(3): 315–319. <https://doi.org/10.1111/j.1096-0031.1994.tb00181.x>
- Graça RN, Alfenas AC, Maffia LA, Titon M, Alfenas RF, Lau D, Rocabado JMA (2009) Factors influencing infection of eucalypts by *Cylindrocladium pteridis*. *Plant Pathology* 58(5): 971–981. <https://doi.org/10.1111/j.1365-3059.2009.02094.x>
- Guerber JC, Correll JC (2001) Characterization of *Glomerella acutata*, the teleomorph of *Colletotrichum acutatum*. *Mycologia* 93(1): 216–229. <https://doi.org/10.1080/00275514.2001.12063151>
- Hepperle D (2004) SeqAssem. Win32-Version. A sequence analysis tool contig assembler and trace data visualization tool for molecular sequences. Win32-Version. [Distributed by the author via:] <http://www.sequentix.de>
- Hoang DT, Chernomor O, Von Haeseler A, Minh BQ, Vinh LS (2018) UFBoot2: Improving the ultrafast bootstrap approximation. *Molecular Biology and Evolution* 35(2): 518–522. <https://doi.org/10.1093/molbev/msx281>
- Huson DH, Bryant D (2006) Application of phylogenetic networks in evolutionary studies. *Molecular Biology and Evolution* 23(2): 254–267. <https://doi.org/10.1093/molbev/msj030>
- IBÁ (2021) IBÁ—Indústria Brasileira de Árvores. Relatório 2020. <https://iba.org/datafiles/publicacoes/relatorios/relatorio-iba-2020.pdf>
- IEA (2020) IEA—Instituto de Economia Agrícola. <https://www.noticiasagricolas.com.br/cotacoes/silvicultura/preco-eucalipto>
- Kang JC, Crous PW, Schoch CL (2001) Species concepts in the *Cylindrocladium floridanum* and *Cy. spathiphylli* complexes (Hypocreaceae) based on multi-allelic sequence data, sexual compatibility and morphology. *Systematic and Applied Microbiology* 24(2): 206–217. <https://doi.org/10.1078/0723-2020-00026>
- Katoh K, Rozewicki J, Yamada KD (2019) MAFFT online service: Multiple sequence alignment, interactive sequence choice and visualization. *Briefings in Bioinformatics* 20(4): 1160–1166. <https://doi.org/10.1093/bib/bbx108>
- Kumar S, Stecher G, Tamura K (2016) MEGA7: Molecular evolutionary genetics analysis version 7.0 for bigger datasets. *Molecular Biology and Evolution* 33(7): 1870–1874. <https://doi.org/10.1093/molbev/msw054>
- Lee SB, Taylor JW (1990) Isolation of DNA from fungal mycelia and single spores. In: Innis MA, Gelfand DV, Sninsky JJ, White TJ (Eds) PCR protocols: a guide to methods and applications. Academic Press, New York, 282–287. <https://doi.org/10.1016/B978-0-12-372180-8.50038-X>
- Li JQ, Wingfield BD, Wingfield MJ, Barnes I, Fourie A, Crous PW, Chen SF (2020) Mating genes in *Calonectria* and evidence for a heterothallic ancestral state. *Persoonia. Molecular Phylogeny and Evolution of Fungi* 45(1): 163–176. <https://doi.org/10.3767/persoonia.2020.45.06>
- Li JQ, Barnes I, Liu FF, Wingfield MJ, Chen SF (2021) Global genetic diversity and mating type distribution of *Calonectria pauciramosa*: An important wide host-range plant pathogen. *Plant Disease* 105(6): 1648–1656. <https://doi.org/10.1094/PDIS-05-20-1050-RE>
- Liu Q, Chen S (2017) Two novel species of *Calonectria* isolated from soil in a natural forest in China. *MycoKeys* 26: 25–60. <https://doi.org/10.3897/mycokeys.26.14688>

- Liu YJ, Whelen S, Hall BD (1999) Phylogenetic relationships among ascomycetes: Evidence from an RNA polymerase II subunit. *Molecular Biology and Evolution* 16(12): 1799–1808. <https://doi.org/10.1093/oxfordjournals.molbev.a026092>
- Liu QL, Li JQ, Wingfield MJ, Duong TA, Wingfield BD, Crous PW, Chen SF (2020) Reconsideration of species boundaries and proposed DNA barcodes for *Calonectria*. *Studies in Mycology* 97: e100106. [71 pp.] <https://doi.org/10.1016/j.simyco.2020.08.001>
- Liu L, Wu W, Chen S (2021) Species diversity and distribution characteristics of *Calonectria* in five soil layers in a eucalyptus plantation. *Journal of Fungi* (Basel, Switzerland) 7(10): e857. <https://doi.org/10.3390/jof7100857>
- Lombard L, Crous PW, Wingfield BD, Wingfield MJ (2010a) Multigene phylogeny and mating tests reveal three cryptic species related to *Calonectria pauciramosa*. *Studies in Mycology* 66: 15–30. <https://doi.org/10.3114/sim.2010.66.02>
- Lombard L, Crous PW, Wingfield BD, Wingfield MJ (2010b) Phylogeny and systematics of the genus *Calonectria*. *Studies in Mycology* 66: 31–69. <https://doi.org/10.3114/sim.2010.66.03>
- Lombard L, Crous PW, Wingfield BD, Wingfield MJ (2010c) Species concepts in *Calonectria (Cylindrocladum)*. *Studies in Mycology* 66: 1–13. <https://doi.org/10.3114/sim.2010.66.01>
- Lombard L, Wingfield MJ, Alfenas AC, Crous PW (2016) The forgotten *Calonectria* collection: Pouring old wine into new bags. *Studies in Mycology* 85(1): 159–198. <https://doi.org/10.1016/j.simyco.2016.11.004>
- Miranda IDS, Auer CG, dos Santos ÁF, Ferreira MA, Tambarussi EV, da Silva RAF, Rezende EH (2021) Occurrence of *Calonectria* leaf blight in *Eucalyptus benthamii* progenies and potential for disease resistance. *Tropical Plant Pathology* 46(3): 254–264. <https://doi.org/10.1007/s40858-021-00426-4>
- Mohali SR, Stewart JE (2021) *Calonectria viginensis* sp. nov. (Hypocreales, Nectriaceae) associated with dieback and sudden-death symptoms of *Theobroma cacao* from Mérida state, Venezuela. *Botany* 99(11): 683–693. <https://doi.org/10.1139/cjb-2021-0050>
- Nguyen LT, Schmidt HA, Von Haeseler A, Minh BQ (2015) IQ-TREE: A fast and effective stochastic algorithm for estimating maximum-likelihood phylogenies. *Molecular Biology and Evolution* 32(1): 268–274. <https://doi.org/10.1093/molbev/msu300>
- Nylander JAA (2004) MrModeltest v2. Program distributed by the author. Evolutionary Biology Centre, Uppsala University.
- O'Donnell K, Cigelnik E (1997) Two divergent intragenomic rDNA ITS2 types within a monophyletic lineage of the fungus *Fusarium* are nonorthologous. *Molecular Phylogenetics and Evolution* 7(1): 103–116. <https://doi.org/10.1006/mpev.1996.0376>
- O'Donnell K, Kistler HC, Cigelnik E, Ploetz RC (1998) Multiple evolutionary origins of the fungus causing Panama disease of banana: Concordant evidence from nuclear and mitochondrial gene genealogies. *Proceedings of the National Academy of Sciences of the United States of America* 95(5): 2044–2049. <https://doi.org/10.1073/pnas.95.5.2044>
- Pham NQ, Barnes I, Chen S, Liu F, Dang QN, Pham TQ, Lombard L, Crous PW, Wingfield MJ (2019) Ten new species of *Calonectria* from Indonesia and Vietnam. *Mycologia* 111(1): 78–102. <https://doi.org/10.1080/00275514.2018.1522179>

- Pham NQ, Marinowitz S, Chen S, Yaparudin Y, Wingfield MJ (2022) *Calonectria* species, including four novel taxa, associated with *Eucalyptus* in Malaysia. Mycological Progress 21(1): 181–197. <https://doi.org/10.1007/s11557-021-01768-8>
- Pires BM (2000) Efeito da desrama artificial no crescimento e qualidade da madeira de *Eucalyptus grandis* para serraria. MSc Dissertation, Universidade Federal de Viçosa, Viçosa, Brasil. <https://locus.ufv.br//handle/123456789/11170>
- Poltronieri LS, Alfenas RF, Verzignassi JR, Alfenas AC, Benchimol RL, Poltronieri TPDS (2011) Leaf blight and defoliation of *Eugenia* spp. caused by *Cylindrocladium candelabrum* and *C. spathiphylli* in Brazil. Summa Phytopathologica 37(2): 147–149. <https://doi.org/10.1590/S0100-54052011000200011>
- Posada D, Crandall KA (1998) Modeltest: Testing the model of DNA substitution. Bioinformatics (Oxford, England) 14(9): 817–818. <https://doi.org/10.1093/bioinformatics/14.9.817>
- Pulrolnik K, Reis GGD, Reis MDGF, Monte MA, Fontan IDCI (2005) Crescimento de plantas de clones de *Eucalyptus grandis* [Hill ex Maiden] submetidas a diferentes tratamentos de desrama artificial, na região do cerrado. Revista Árvore 29(4): 495–505. <https://doi.org/10.1590/S0100-67622005000400001>
- Quaedvlieg W, Kema GHJ, Groenewald JZ, Verkley GJM, Seifbarghi S, Razavi M, Gohari AM, Mehrabi R, Crous PW (2011) *Zymoseptoria* gen. nov.: A new genus to accommodate *Septoria*-like species occurring on graminicolous hosts. Persoonia. Molecular Phylogeny and Evolution of Fungi 26(1): 57–69. <https://doi.org/10.3767/003158511X571841>
- Rambaut A (2009) FigTree, a graphical viewer of phylogenetic trees. <http://tree.bio.ed.ac.uk/software/figtree/>
- Rambaut A, Drummond AJ (2007) Tracer v1.5. <http://tree.bio.ed.ac.uk/software/tracer/>
- Reeb V, Lutzoni F, Roux C (2004) Contribution of RPB2 to multilocus phylogenetic studies of the euascomycetes (Pezizomycotina, Fungi) with special emphasis on the lichen-forming Acarosporaceae and evolution of polyspority. Molecular Phylogenetics and Evolution 32(3): 1036–1060. <https://doi.org/10.1016/j.ympev.2004.04.012>
- Reis A, Mafia RG, Silva PP, Lopes CA, Alfenas AC (2004) *Cylindrocladium spathiphylli*, causal agent of *Spathiphyllum* root and collar rot in the Federal District-Brazil. Fitopatologia Brasileira 29(1): 102–102. <https://doi.org/10.1590/S0100-41582004000100017>
- Ronquist F, Teslenko M, Van Der Mark P, Ayres DL, Darling A, Höhna S, Larget B, Liu L, Suchard MA, Huelsenbeck JP (2012) MrBayes 3.2: Efficient Bayesian phylogenetic inference and model choice across a large model space. Systematic Biology 61(3): 539–542. <https://doi.org/10.1093/sysbio/sys029>
- Ronquist F, Huelsenbeck J, Teslenko M, Nylander JAA (2019) MrBayes version 3.2 manual: tutorials and model summaries. <https://nbisweden.github.io/MrBayes/manual.html>
- Schoch CL, Crous PW, Wingfield BD, Wingfield MJ (1999) The *Cylindrocladium candelabrum* species complex includes four distinct mating populations. Mycologia 91(2): 286–298. <https://doi.org/10.1080/00275514.1999.12061019>
- Soares TP, Pozza EA, Pozza AA, Mafia RG, Ferreira MA (2018) Calcium and potassium imbalance favours leaf blight and defoliation caused by *Calonectria pteridis* in *Eucalyptus* plants. Forests 9(12): e782. <https://doi.org/10.3390/f9120782>

- Sullivan J (1996) Combining data with different distributions of among-site rate variation. *Systematic Biology* 45(3): 375–380. <https://doi.org/10.1093/sysbio/45.3.375>
- Swofford DL (2003) PAUP*. Phylogenetic analysis using parsimony (*and other methods). V. 4.0b10. Sinauer Associates, Sunderland, Massachusetts, USA.
- Taylor JW, Jacobson DJ, Kroken S, Kasuga T, Geiser DM, Hibbett DS, Fisher MC (2000) Phylogenetic species recognition and species concepts in fungi. *Fungal Genetics and Biology* 31(1): 21–32. <https://doi.org/10.1006/fgb.2000.1228>
- Trifinopoulos J, Nguyen LT, von Haeseler A, Minh BQ (2016) W-IQ-TREE: A fast online phylogenetic tool for maximum likelihood analysis. *Nucleic Acids Research* 44(W1): W232–W235. <https://doi.org/10.1093/nar/gkw256>
- Vitale A, Crous PW, Lombard L, Polizzi G (2013) *Calonectria* diseases on ornamental plants in Europe and the Mediterranean basin: An overview. *Journal of Plant Pathology* 95(3): 463–476. <https://doi.org/10.4454/JPP.V95I3.007>
- Wang QC, Liu QL, Chen SF (2019) Novel species of *Calonectria* isolated from soil near *Eucalyptus* plantations in southern China. *Mycologia* 111(6): 1028–1040. <https://doi.org/10.1080/00275514.2019.1666597>
- Wingfield MJ, Brockerhoff EG, Wingfield BD, Slippers B (2015) Planted forest health: The need for a global strategy. *Science* 349(6250): 832–836. <https://doi.org/10.1126/science.aac6674>

Supplementary material I

Figures S1–S6

Authors: Enrique I. Sanchez-Gonzalez, Thaissa de Paula Farias Soares, Talyta Galafassi Zarpelon, Edival Angelo Valverde Zauza, Reginaldo Gonçalves Mafia, Maria Alves Ferreira
Data type: Phylogenetic trees (pdf file)

Explanation note: **Figure S1.** Phylogenetic tree based on maximum likelihood analysis of *act* gene region. Bootstrap support values $\geq 80\%$ for maximum parsimony (MP), Ultrafast bootstrap support values $\geq 95\%$ for maximum likelihood (ML), and posterior probability (PP) values ≥ 0.95 from BI analyses are presented at the nodes (MP/ML/PP). Bootstrap values below 80% (MP), 95% (ML) and posterior probabilities below 0.80 are marked with “-”. Ex-type isolates are indicated by “▲”, isolates highlighted in bold were sequenced in this study, and novel species are in blue and orange. *C. gracilipes* was used as outgroup. The scale bar indicates the number of nucleotide substitutions per site. **Figure S2.** Phylogenetic tree based on maximum likelihood analysis of *cmdA* gene region. Bootstrap support values $\geq 80\%$ for maximum parsimony (MP), Ultrafast bootstrap support values $\geq 95\%$ for maximum likelihood (ML), and posterior probability (PP) values ≥ 0.95 from BI analyses are presented at the nodes (MP/ML/PP). Bootstrap values below 80% (MP), 95% (ML) and posterior probabilities below 0.80 are marked with “-”. Ex-type isolates are indicated by “▲”, isolates highlighted in bold were sequenced

in this study, and novel species are in blue and orange. *C. gracilipes* was used as outgroup. The scale bar indicates the number of nucleotide substitutions per site.

Figure S3. Phylogenetic tree based on maximum likelihood analysis of *bis3* gene region. Bootstrap support values $\geq 80\%$ for maximum parsimony (MP), Ultrafast bootstrap support values $\geq 95\%$ for maximum likelihood (ML), and posterior probability (PP) values ≥ 0.95 from BI analyses are presented at the nodes (MP/ML/PP). Bootstrap values below 80% (MP), 95% (ML) and posterior probabilities below 0.80 are marked with “-”. Ex-type isolates are indicated by “▲”, isolates highlighted in bold were sequenced in this study, and novel species are in blue and orange. *C. gracilipes* was used as outgroup. The scale bar indicates the number of nucleotide substitutions per site. **Figure S4.** Phylogenetic tree based on maximum likelihood analysis of *rpb2* gene region. Bootstrap support values $\geq 80\%$ for maximum parsimony (MP), Ultrafast bootstrap support values $\geq 95\%$ for maximum likelihood (ML), and posterior probability (PP) values ≥ 0.95 from BI analyses are presented at the nodes (MP/ML/PP). Bootstrap values below 80% (MP), 95% (ML) and posterior probabilities below 0.80 are marked with “-”. Ex-type isolates are indicated by “▲”, isolates highlighted in bold were sequenced in this study, and novel species are in blue and orange. *C. gracilipes* was used as outgroup. The scale bar indicates the number of nucleotide substitutions per site. **Figure S5.** Phylogenetic tree based on maximum likelihood analysis of *tef1* gene region. Bootstrap support values $\geq 80\%$ for maximum parsimony (MP), Ultrafast bootstrap support values $\geq 95\%$ for maximum likelihood (ML), and posterior probability (PP) values ≥ 0.95 from BI analyses are presented at the nodes (MP/ML/PP). Bootstrap values below 80% (MP), 95% (ML) and posterior probabilities below 0.80 are marked with “-”. Ex-type isolates are indicated by “▲”, isolates highlighted in bold were sequenced in this study, and novel species are in blue and orange. *C. gracilipes* was used as outgroup. The scale bar indicates the number of nucleotide substitutions per site.

Figure S6. Phylogenetic tree based on maximum likelihood analysis of *tub2* gene region. Bootstrap support values $\geq 80\%$ for maximum parsimony (MP), Ultrafast bootstrap support values $\geq 95\%$ for maximum likelihood (ML), and posterior probability (PP) values ≥ 0.95 from BI analyses are presented at the nodes (MP/ML/PP). Bootstrap values below 80% (MP), 95% (ML) and posterior probabilities below 0.80 are marked with “-”. Ex-type isolates are indicated by “▲”, isolates highlighted in bold were sequenced in this study, and novel species are in blue and orange. *C. gracilipes* was used as outgroup. The scale bar indicates the number of nucleotide substitutions per site.

Copyright notice: This dataset is made available under the Open Database License (<http://opendatacommons.org/licenses/odbl/1.0/>). The Open Database License (ODbL) is a license agreement intended to allow users to freely share, modify, and use this Dataset while maintaining this same freedom for others, provided that the original source and author(s) are credited.

Link: <https://doi.org/10.3897/mycokeys.91.84896.suppl1>